

A priori and *a posteriori* error analysis for the Nitsche's method of a reduced Landau-de Gennes problem

Ruma Rani Maity* Apala Majumdar* † Neela Nataraj‡

February 28, 2022

Abstract

The equilibrium configurations of a two dimensional planar bistable nematic liquid crystal device are modelled by a system of second order semi-linear elliptic partial differential equations with non-homogeneous boundary conditions. In this article, Nitsche's method is applied to approximate the solution of this non-linear model. A discrete inf-sup condition sufficient for the stability of a well-posed linear problem is established and this with a fixed point theorem allows the proof of local existence and uniqueness of a discrete solution to the semi-linear problems. *A priori* and *a posteriori* energy norm analysis is established for a sufficiently large penalization parameter and sufficiently fine triangulation. Optimal order *a priori* error estimates in L^2 norm is also established. Several numerical examples that confirm the theoretical results are presented.

Keywords: Landau-de Gennes energy functional, non-linear elliptic pde, non-homogeneous Dirichlet boundary data, lower regularity, Nitsche's method, *a priori* and *a posteriori* error estimates, adaptive finite element methods

1 Introduction

In this paper, we derive *a priori* and *a posteriori* estimates for a system of partial differential equations that arise naturally in different contexts for two-dimensional systems, our primary motivation being two-dimensional liquid crystal systems [18]. Liquid crystals are intermediate phases of matter between the conventional solid and liquid states of matter with versatile properties of both phases. This makes them ubiquitous and we focus on nematic liquid crystals for which the constituent rod-like molecules translate freely but exhibit locally preferred directions of orientational ordering, referred to as nematic directors [18]. There are at least three well-known mathematical theories for nematic liquid crystals in the literature: the Oseen-Frank model [1, 4, 35], Ericksen model [21] and the most general Landau-De Gennes model [17, 19, 40].

In the Landau-de Gennes theory, the state of a nematic liquid crystal is described by the Q -tensor order parameter: a symmetric traceless 3×3 matrix that contains information about the nematic directors and the degree of orientational ordering about them [40]. We work within a reduced Landau-de Gennes framework which has been rigorously justified for two-dimensional domains [24, 47], for certain model situations. In the reduced case, the order parameter is a symmetric, traceless 2×2 matrix which can be written as $Q := s(2\mathbf{n} \otimes \mathbf{n} - I)$, with $Q \in \mathbf{S}_0 := \{Q = (Q_{ij})_{1 \leq i, j \leq 2} \in \mathbb{R}^{2 \times 2} : Q = Q^T, \text{tr}Q = 0\}$ and I is the 2×2 identity matrix. The locally preferred in-plane nematic director ' \mathbf{n}' ', can be parameterized by an angle θ in the plane as $\mathbf{n} = (\cos \theta, \sin \theta)$ and the scalar order parameter s measures the degree of order about ' \mathbf{n}' '. Since Q is a symmetric, traceless 2×2 matrix, we can write it as $\Psi = (u, v)$ where $u = s \cos 2\theta$ and $v = s \sin 2\theta$. The stable nematic equilibria are minimizers of a Landau-de Gennes energy, for example

$$\mathcal{E}(Q) := \mathcal{E}_B(Q) + \mathcal{E}_E(Q) + \mathcal{E}_S(Q) - \mathcal{E}_L(Q)$$

*Department of Mathematics, Indian Institute of Technology Bombay, Powai, Mumbai 400076, India. Email. ruma@math.iitb.ac.in

†* Department of Mathematics And Statistics, University of Strathclyde, 16 Richmond St, Glasgow G1 1XQ, United Kingdom. Visiting Professor, Indian Institute of Technology Bombay, Powai, Mumbai 400076, India. Email. apala.majumdar@strath.ac.uk

‡Department of Mathematics, Indian Institute of Technology Bombay, Powai, Mumbai 400076, India. Email. neela@math.iitb.ac.in

subject to appropriate boundary conditions [17]. The bulk energy $\mathcal{E}_B(Q)$ drives the first order isotropic-nematic transition in spatially homogeneous samples as a function of the temperature. There are different forms of the elastic energy but we employ the one-constant elastic energy: $\mathcal{E}_E(Q) := \int_{\Omega} \frac{L_{el}}{2} |\nabla Q|^2 dx$ with $L_{el} > 0$ being an elastic constant. The surface anchoring energy accounts for the imposed boundary conditions, $\mathcal{E}_S(Q) := \int_{\partial\Omega} W|(Q_{11}, Q_{12}) - \mathbf{g}|^2 ds$ where $W > 0$ is the anchoring strength on $\partial\Omega$ and $\mathbf{g} : \partial\Omega \rightarrow \mathbb{R}^2$ is a prescribed preferred Lipschitz continuous boundary condition. In the limit $W \rightarrow \infty$, we recover the Dirichlet conditions $Q = \mathbf{g}$ on $\partial\Omega$. The electrostatic energy accounts for the effect of external fields i.e. the coupling between the nematic directors and the external electric field or magnetic field.

For Dirichlet conditions and in the absence of external fields, the dimensionless reduced Landau-de Gennes free energy [37] can be written as

$$\mathcal{E}(\Psi_{\epsilon}) = \int_{\Omega} (|\nabla \Psi_{\epsilon}|^2 + \epsilon^{-2} (|\Psi_{\epsilon}|^2 - 1)^2) dx, \quad (1.1)$$

where we take Ω to be an open and bounded domain in \mathbb{R}^2 with polygonal boundary $\partial\Omega$, $\Psi_{\epsilon} = \mathbf{g}$ on $\partial\Omega$ and ϵ is a material-dependent parameter that depends on the elastic constant, domain size and temperature. Informally speaking, $\epsilon \propto \sqrt{\frac{L_{el}}{|A|}} * \frac{1}{D}$, where D is a characteristic domain size.

The corresponding Euler-Lagrange equations are a system of second order non-linear elliptic partial differential equations (PDEs) and the critical points (including energy minimizers), $\Psi_{\epsilon} \in \mathbf{H}^1(\Omega)$, are weak solutions of

$$-\Delta \Psi_{\epsilon} = 2\epsilon^{-2}(1 - |\Psi_{\epsilon}|^2)\Psi_{\epsilon} \text{ in } \Omega \text{ and } \Psi_{\epsilon} = \mathbf{g} \text{ on } \partial\Omega. \quad (1.2)$$

Define the admissible space $\mathcal{X} = \{\mathbf{w} \in \mathbf{H}^1(\Omega) : \mathbf{w} = \mathbf{g} \text{ on } \partial\Omega\}$. In what follows, we work with fixed but small values of ϵ which describe large domains for which $D \gg \sqrt{\frac{L_{el}}{|A|}}$, and $\sqrt{\frac{L_{el}}{|A|}}$ is proportional to the nematic correlation length associated with nematic defect core sizes [27]. The non-linear system (1.2) is in fact the Ginzburg-Landau model with a rescaled ϵ , which has been extensively studied in [7, 8, 42]. There are several powerful analytic results on the asymptotic behavior of solutions, Ψ_{ϵ} as $\epsilon \rightarrow 0$, and their defects, known as Ginzburg-Landau vortices, along with their dependence on the topology of the domain and the boundary data. This model has been applied with success to the planar bistable nematic device reported in [45] where the authors study nematic liquid crystals-filled shallow square wells, with experimentally imposed tangent boundary conditions, and report the existence of diagonal and rotated solutions. The nematic director is aligned along the square diagonals in the diagonal solutions, and rotates by π radians for the rotated solutions. There are two rotationally equivalent diagonal solutions and four rotationally equivalent rotated solutions. In [37], the authors report interesting numerical convergence results for the diagonal and rotated solutions, in a conforming finite-element set-up, as a function of ϵ .

In [39], the authors carry out a rigorous *a priori* error analysis for the discontinuous Galerkin finite element (dGFEM) approximation of \mathbf{H}^2 -regular solutions of (1.2) in *convex polygonal* domains. The authors present a convergence analysis for the optimal linear (resp. quadratic) order of convergence in energy (resp. \mathbf{L}^2) norm for solutions, $\Psi_{\epsilon} \in \mathbf{H}^2(\Omega)$ with an analysis of the $h - \epsilon$ dependency, where h is the mesh size or the discretization parameter, accompanied by some numerical experiments in the context of the planar bistable nematic device in the dGFEM framework. However, *a posteriori* error estimates for (1.2) are **not studied** in [39].

In this paper, we apply Nitsche's finite-element approximation method to the system (1.2), with non-homogeneous Dirichlet conditions \mathbf{g} on a two-dimensional bounded domain Ω . Our main contribution is to relax the regularity assumptions on Ψ_{ϵ} as will be explained below, so that the analysis extends to convex and non-convex domains with polygonal boundaries, and to Dirichlet data of low regularity. The Nitsche's method is well-studied in the literature; it was first applied to the Poisson's problem with non-homogeneous boundary conditions in [41]. Juntunen et al. [28] extended the method for general Robin boundary conditions and discussed *a priori* and *a posteriori* error analysis when the exact solution belongs to $H^s(\Omega)$ with $s > \frac{3}{2}$. An improved *a priori* error analysis for Nitsche's method, without the regularity assumption $s > 3/2$, has been derived in [38] using the medius analysis [26].

There are also extensive results for the *a posteriori* analysis of the Poisson problem, see for example, [9, 12, 28, 32]. An *a posteriori* error analysis for the mixed formulation of Poisson equation with homogeneous

boundary conditions is discussed in [9] with a *saturation assumption* that can be stated as the approximate solution of the problem in a finer mesh constitutes a better approximation to the exact solution than the one in a coarser mesh in the energy norm. Similar saturation assumptions are utilised in [28] for the Nitsche's method for Poisson equation. *A posteriori* error bounds for finite element methods for Poisson problem with mixed boundary conditions and C^0 -Dirichlet boundary condition are studied in [5, 12] without saturation assumptions. A residual-type error estimator for a locally conservative mixed method for Poisson problem with non-homogeneous C^0 -Dirichlet boundary conditions, without saturation assumption, is studied in [32]. *A priori* and *a posteriori* error analysis of dGFEMs for the von Kármán equations are studied in [14].

The convergence analysis in [39] for the dGFEM assumes that the exact solution belongs to $\mathbf{H}^2(\Omega)$. The first challenge with a less regular solution $\Psi_\epsilon \in \mathcal{X} \cap \mathbf{H}^{1+\alpha}(\Omega)$, where $\alpha \in (0, 1)$ is the index of elliptic regularity [25], is to handle the normal derivatives $\nabla \Psi_{\epsilon\nu} \notin \mathbf{L}^2(E)$ across the element boundaries E , for both Nitsche's method and dGFEM. In this paper, we overcome this by employing the medius analysis [26] that combines ideas of both *a posteriori* and *a priori* analysis. We apply the Nitsche's method to a semi-linear problem with cubic nonlinearity and non-homogeneous Dirichlet boundary conditions in (1.2) for the first time and utilize the medius analysis for the relevant *a priori* estimates. Our *first* contribution is a rigorous *a priori* finite-element error analysis for (1.2) using the Nitsche's method to incorporate the non-homogeneous boundary conditions. This includes solutions with lesser regularity than $\mathbf{H}^{3/2}(\Omega)$, i.e. solutions in the space $\mathcal{X} \cap \mathbf{H}^{1+\alpha}(\Omega)$ where $\alpha \in (0, 1]$.

The reduced regularity assumption for the exact solution is relevant for non-convex polygons with $\alpha < 1$ [25]. Further, the convergence for a quasi-uniform triangulation with maximal mesh-size h is not better than h^α so that adaptive mesh-refinement is desirable. It is now well-established that *a posteriori* error estimators provide a systematic way of controlling errors and are an indispensable tool for performing adaptive mesh refinements [2, 46]. Given this motivation, our *second* contribution is a reliable and efficient residual type *a posteriori* error estimate for (1.2). The non-homogeneous boundary function $\mathbf{g} \in \mathbf{H}^{1/2}(\partial\Omega)$ is assumed to be in $\mathbf{C}^0(\partial\Omega)$ and the Helmholtz decomposition technique [32, 33] is exploited to derive the estimators. These reliable and efficient *a posteriori* estimates enable local refinements and the adaptive mesh algorithm captures the numerical errors near regions of high distortion or large $|\nabla \Psi_\epsilon|$, typically the zero set of the solution or near the corners of the two-dimensional domain through local refinements.

Additionally, we conduct several numerical experiments for uniform as well as adaptive refinement that not only validate the theoretical estimates for both *a priori* and *a posteriori* error analysis but also clearly illustrate the advantages of adaptive FEMs. The numerical experiment in [39, Example 6.2.2] implies that the errors are sensitive to the choice of the discretization parameter as $\epsilon \rightarrow 0$, and smaller mesh sizes are needed for convergence. This is computationally expensive for uniform mesh refinements while adaptive mesh refinement significantly reduces the computational cost, by requiring the discretization parameter h to be small only near suitably identified regions. Indeed, the convergence of the discrete solutions to the exact solution is faster with adaptive refinement. Our analysis is restricted to a small but a fixed value of ϵ and we present informative convergence plots, in terms of number of degrees of freedom, for adaptive refinements in different polygonal domains. These results have applications to model liquid crystal problems on non-convex domains or domains with re-entrant corners, or with Dirichlet data of low regularity.

We use the usual notation for Sobolev spaces $H^s(\Omega)$ (resp. $W^{s,p}(\Omega)$) with s, p positive real numbers, equipped with the usual norms $\|\cdot\|_s$ (resp. $\|\cdot\|_{s,p}$). The space $\mathbf{H}^s(\Omega)$ (resp. $\mathbf{L}^p(\Omega)$) is defined to be the product space $H^s(\Omega) \times H^s(\Omega)$ (resp. $L^p(\Omega) \times L^p(\Omega)$) equipped with the corresponding norms $\|\cdot\|_s$ (resp. $\|\cdot\|_{s,p}$) defined by $\|\Phi\|_s = (\|\varphi_1\|_s^2 + \|\varphi_2\|_s^2)^{1/2}$ for all $\Phi = (\varphi_1, \varphi_2) \in \mathbf{H}^s(\Omega)$ (resp. $\|\Phi\|_{s,p} = (\|\varphi_1\|_{s,p}^2 + \|\varphi_2\|_{s,p}^2)^{1/2}$ for all $\Phi = (\varphi_1, \varphi_2) \in \mathbf{W}^{s,p}(\Omega)$). The norm on $\mathbf{L}^2(\Omega)$ space is simply $\|\Phi\|_0 = (\|\varphi_1\|_0^2 + \|\varphi_2\|_0^2)^{1/2}$ for all $\Phi = (\varphi_1, \varphi_2) \in \mathbf{L}^2(\Omega)$. Set $\mathbf{V} := H_0^1(\Omega) = \left\{ \phi \in L^2(\Omega) : \frac{\partial \phi}{\partial x}, \frac{\partial \phi}{\partial y} \in L^2(\Omega), \phi|_{\partial\Omega} = 0 \right\}$ and $\mathbf{V} = \mathbf{H}_0^1(\Omega) = H_0^1(\Omega) \times H_0^1(\Omega)$. As per standard convention $a \lesssim b \iff a \leq Cb$ where the constant C is independent of the discretization parameter h . We use C_s to denote a generic constant, containing different Sobolev imbedding constants, throughout the manuscript.

Our paper is organized as follows. In the next section, we define the discrete space, review Nitsche's method and the discrete problem. Subsection 2.3 is devoted to the main results for both *a priori* and *a posteriori* error analysis, followed by some auxiliary results needed for the key proofs. Subsection 3.2 focuses on the rigorous *a priori* error estimates along with some numerical experiments that confirm the theoretical estimates in Subsection 3.3. We present a reliable and efficient *a posteriori* error analysis in Section 4 followed by a set of numerical experiments to validate the theoretical results. Section 5 concludes

with some brief perspectives. The Appendix contains the proofs of regularity and local efficiency estimates.

2 Preliminaries and main results

The weak formulation of the non-linear system (1.2), the basics of the Nitsche's method and the main results of the paper are stated in this section.

2.1 Weak formulations

The weak formulation of (1.2) can be stated as follows: we seek $\Psi_\epsilon \in \mathcal{X}$ such that

$$N(\Psi_\epsilon; \Phi) := A(\Psi_\epsilon, \Phi) + B(\Psi_\epsilon, \Psi_\epsilon, \Psi_\epsilon, \Phi) + C(\Psi_\epsilon, \Phi) = 0 \quad \text{for all } \Phi \in \mathbf{V}, \quad (2.1)$$

where for all $\Xi = (\xi_1, \xi_2)$, $\boldsymbol{\eta} = (\eta_1, \eta_2)$, $\Theta = (\theta_1, \theta_2)$, $\Phi = (\varphi_1, \varphi_2) \in \mathbf{X} := \mathbf{H}^1(\Omega)$,

$$\begin{aligned} A(\Theta, \Phi) &:= a(\theta_1, \varphi_1) + a(\theta_2, \varphi_2), \quad C(\Theta, \varphi) := c(\theta_1, \varphi_1) + c(\theta_2, \varphi_2), \\ B(\Xi, \boldsymbol{\eta}, \Theta, \Phi) &:= \frac{2}{3\epsilon^2} \int_{\Omega} ((\Xi \cdot \boldsymbol{\eta})(\Theta \cdot \Phi) + 2(\Xi \cdot \Theta)(\boldsymbol{\eta} \cdot \Phi)) \, dx = \frac{1}{3} (3b(\xi_1, \eta_1, \theta_1, \varphi_1) + 3b(\xi_2, \eta_2, \theta_2, \varphi_2) \\ &\quad + 2b(\xi_2, \eta_1, \theta_2, \varphi_1) + 2b(\xi_1, \eta_2, \theta_1, \varphi_2) + b(\xi_2, \eta_2, \theta_1, \varphi_1) + b(\xi_1, \eta_1, \theta_2, \varphi_2)), \end{aligned}$$

$$\text{and for } \xi, \eta, \theta, \varphi \in H^1(\Omega), \quad a(\theta, \varphi) := \int_{\Omega} \nabla \theta \cdot \nabla \varphi \, dx, \quad b(\xi, \eta, \theta, \varphi) := 2\epsilon^{-2} \int_{\Omega} \xi \eta \theta \varphi \, dx$$

$$\text{and } c(\theta, \varphi) := -2\epsilon^{-2} \int_{\Omega} \theta \varphi \, dx.$$

See [37, 39] for a proof of existence of minimizers of the Landau-de Gennes energy functional (1.1) that are solutions to (2.1). In this article, we investigate cases of lower regularity, for example when the domain is a non-convex polygon and the solution of (2.1) belongs to $\mathcal{X} \cap \mathbf{H}^{1+\alpha}(\Omega)$, and the index of elliptic-regularity $\alpha \in (0, 1)$, for details see Appendix A.2. When Ω is a convex polygon, $\alpha = 1$; that is, the solution of (2.1) belongs to $\mathcal{X} \cap \mathbf{H}^2(\Omega)$.

In this paper, we approximate the regular (also referred to as non-singular in literature) solutions [30], Ψ_ϵ of (1.2) for a fixed ϵ . This implies that the linearized operator $\langle DN(\Psi_\epsilon) \cdot, \cdot \rangle$ is invertible in the Banach space and is equivalent to the following inf-sup conditions [20]

$$0 < \beta := \inf_{\substack{\Theta \in \mathbf{V} \\ \|\Theta\|_1=1}} \sup_{\substack{\Phi \in \mathbf{V} \\ \|\Phi\|_1=1}} \langle DN(\Psi_\epsilon)\Theta, \Phi \rangle, \quad \text{and } 0 < \beta = \inf_{\substack{\Phi \in \mathbf{V} \\ \|\Phi\|_1=1}} \sup_{\substack{\Theta \in \mathbf{V} \\ \|\Theta\|_1=1}} \langle DN(\Psi_\epsilon)\Theta, \Phi \rangle, \quad (2.2)$$

where $\langle DN(\Psi_\epsilon)\Theta, \Phi \rangle := A(\Theta, \Phi) + 3B(\Psi_\epsilon, \Psi_\epsilon, \Theta, \Phi) + C(\Theta, \Phi)$ and the inf-sup constant β depends on ϵ . Here and throughout the paper, $\langle \cdot, \cdot \rangle$ denotes the duality pairing between \mathbf{V}^* and \mathbf{V} . The parameter ϵ in Ψ_ϵ is suppressed in the sequel for notational brevity and is chosen fixed in the sequel.

2.2 Nitsche's method

Consider a shape regular triangulation \mathcal{T} of Ω into triangles [16]. Define the mesh discretization parameter $h = \max_{T \in \mathcal{T}} h_T$, where $h_T = \text{diam}(T)$. Denote \mathcal{E}_h^i (resp. \mathcal{E}_h^∂) to be the interior (resp. boundary) edges of \mathcal{T} and let $\mathcal{E} := \mathcal{E}_h^i \cup \mathcal{E}_h^\partial$. The length of an edge E is denoted by h_E . Define the finite element subspace of \mathbf{X} by $\mathbf{X}_h := X_h \times X_h$ with $X_h := \{v \in H^1(\Omega) \mid v|_T \in P_1(T) \text{ for all } T \in \mathcal{T}\}$ along with the discrete norm defined by

$$\|v\|_h^2 := \int_{\Omega} |\nabla v|^2 \, dx + \sum_{E \in \mathcal{E}_h^\partial} \frac{\sigma}{h_E} \int_E v^2 \, ds \quad \text{for all } v \in X_h.$$

Here $\sigma > 0$ is the penalty parameter and $P_1(T)$ is the space of polynomials of degree less than or equal to 1 defined on T . The space \mathbf{X}_h is equipped with the product norm $\|\Phi_h\|_h := \left(\|\varphi_1\|_h^2 + \|\varphi_2\|_h^2 \right)^{1/2}$ for all $\Phi_h = (\varphi_1, \varphi_2) \in \mathbf{X}_h$. Define $\|\Phi_h\|_{0,E}^2 := \|\varphi_1\|_{0,E}^2 + \|\varphi_2\|_{0,E}^2$ and $\|\Phi_h\|_{0,T}^2 := \|\varphi_1\|_{0,T}^2 + \|\varphi_2\|_{0,T}^2$ for $\Phi_h \in \mathbf{X}_h$

such that for $v \in X_h$, $\|v\|_{0,E}^2 := \int_E v^2 ds$ and $\|v\|_{0,T}^2 := \int_T v^2 dx$, respectively. For an interior edge E shared by the triangles T^+ and T^- , define the jump and average of $\varphi \in H^1(\Omega)$ across E as $[\varphi] := \varphi|_{T^+} - \varphi|_{T^-}$ and $\{\varphi\} := \frac{1}{2}(\varphi|_{T^+} + \varphi|_{T^-})$, respectively. For a vector function jump and average are defined component-wise.

For $\Xi = (\xi_1, \xi_2)$, $\eta = (\eta_1, \eta_2)$, $\Theta = (\theta_1, \theta_2)$, $\Phi = (\varphi_1, \varphi_2) \in \mathbf{X}$, define

$$\begin{aligned} A_h(\Theta, \Phi) &:= a_h(\theta_1, \varphi_1) + a_h(\theta_2, \varphi_2), C_h(\Theta, \Phi) := c_h(\theta_1, \varphi_1) + c_h(\theta_2, \varphi_2), L_h(\Phi_h) = l_h^1(\varphi_1) + l_h^2(\varphi_2), \\ B_h(\Xi, \eta, \Theta, \Phi) &:= \frac{2}{3\epsilon^2} \sum_{T \in \mathcal{T}} \int_T ((\Xi \cdot \eta)(\Theta \cdot \Phi) + 2(\Xi \cdot \Theta)(\eta \cdot \Phi)) dx \\ &= \frac{1}{3}(3b_h(\xi_1, \eta_1, \theta_1, \varphi_1) + 3b_h(\xi_2, \eta_2, \theta_2, \varphi_2) + 2b_h(\xi_2, \eta_1, \theta_2, \varphi_1) + 2b_h(\xi_1, \eta_2, \theta_1, \varphi_2) \\ &\quad + b_h(\xi_2, \eta_2, \theta_1, \varphi_1) + b_h(\xi_1, \eta_1, \theta_2, \varphi_2)), \end{aligned} \quad (2.3)$$

and for $\theta, \varphi \in H^1(\Omega)$, $\mathbf{g} = (g_1, g_2)$ and the penalty parameter $\sigma > 0$,

$$\begin{aligned} a_h(\theta, \varphi) &:= \sum_{T \in \mathcal{T}} \int_T \nabla \theta \cdot \nabla \varphi dx - \sum_{E \in \mathcal{E}_h^\partial} \langle \frac{\partial \theta}{\partial \nu}, \varphi \rangle_E - \sum_{E \in \mathcal{E}_h^\partial} \langle \theta, \frac{\partial \varphi}{\partial \nu} \rangle_E + \sum_{E \in \mathcal{E}_h^\partial} \frac{\sigma}{h_E} \langle \theta, \varphi \rangle_E, \\ b_h(\xi, \eta, \theta, \varphi) &:= 2\epsilon^{-2} \sum_{T \in \mathcal{T}} \int_T \xi \eta \theta \varphi dx, \quad c_h(\theta, \varphi) := -2\epsilon^{-2} \sum_{T \in \mathcal{T}} \int_T \theta \varphi dx, \\ \text{and } l_h^i(\varphi) &:= - \sum_{E \in \mathcal{E}_h^\partial} \langle g_i, \frac{\partial \varphi}{\partial \nu} \rangle_E + \sum_{E \in \mathcal{E}_h^\partial} \frac{\sigma}{h_E} \langle g_i, \varphi \rangle_E \text{ for } 1 \leq i \leq 2. \end{aligned}$$

In the sequel, $\langle \cdot, \cdot \rangle_E$ is the duality pairing between $H^{-\frac{1}{2}}(E)$ and $H^{\frac{1}{2}}(E)$ [36] and ν denotes the outward unit normal associated to each edge $E \in \mathcal{E}_h^\partial$. The Nitsche's method corresponding to (1.2) seeks $\Psi_h \in \mathbf{X}_h$, such that for all $\Phi_h \in \mathbf{X}_h$,

$$N_h(\Psi_h; \Phi_h) := A_h(\Psi_h, \Phi_h) + B_h(\Psi_h, \Psi_h, \Psi_h, \Phi_h) + C_h(\Psi_h, \Phi_h) - L_h(\Phi_h) = 0. \quad (2.4)$$

Remark 2.1. The restrictions of the bilinear and quadrilinear forms $C_h(\cdot, \cdot)$, $B_h(\cdot, \cdot, \cdot, \cdot)$ to $T \in \mathcal{T}$ are denoted as $C_T(\cdot, \cdot)$, $B_T(\cdot, \cdot, \cdot, \cdot)$, respectively. Define the bilinear form $A_T(\Theta, \Phi) := \int_T \nabla \Theta \cdot \nabla \Phi dx$ for all $\Theta, \Phi \in \mathbf{X}$. For $\Phi_h = (\varphi_1, \varphi_2) \in \mathbf{X}_h$, let $\nabla \Phi_h \nu := (\frac{\partial \varphi_1}{\partial \nu}, \frac{\partial \varphi_2}{\partial \nu})$ on an edge E with outward unit normal ν to E .

2.3 Main results

The main results in this manuscript are stated in this sub-section. We establish the $O(h^\alpha)$ (resp. $O(h^{2\alpha})$) convergence in energy (resp. $\mathbf{L}^2(\Omega)$) norms, respectively when the exact solution has the regularity $\mathcal{X} \cap \mathbf{H}^{1+\alpha}(\Omega)$, $0 < \alpha < 1$, accompanied by *a posteriori* error estimates.

Theorem 2.2. (A priori error estimate) *Let Ψ be a regular solution of (2.1). For a sufficiently large penalty parameter $\sigma > 0$ and a sufficiently small discretization parameter h , there exists a unique solution Ψ_h to the discrete problem (2.4) that approximates Ψ such that*

$$(i) \quad \|\Psi - \Psi_h\|_h \lesssim h^\alpha, \quad (ii) \quad \|\Psi - \Psi_h\|_0 \lesssim h^{2\alpha},$$

where $\alpha \in (0, 1]$ denotes the index of elliptic regularity.

A reliable and efficient *a posteriori* error estimate for (2.4) is the second main result of the paper. For each element $T \in \mathcal{T}$ and edge $E \in \mathcal{E}$, define the volume and edge contributions to the estimators by

$$\vartheta_T^2 := h_T^2 \|\| 2\epsilon^{-2} (|\Psi_h|^2 - 1) \Psi_h \|_{0,T}^2, \quad (\vartheta_E^i)^2 := h_E \|\| [\nabla \Psi_h \nu] \|_{0,E}^2 \text{ for all } E \in \mathcal{E}_h^i, \quad (2.5)$$

$$\text{and } (\vartheta_E^\partial)^2 := \frac{1}{h_E} \|\| \Psi_h - \mathbf{g} \|_{0,E}^2 \text{ for all } E \in \mathcal{E}_h^\partial. \quad (2.6)$$

Define the estimator

$$\vartheta^2 := \sum_{T \in \mathcal{T}} \vartheta_T^2 + \sum_{E \in \mathcal{E}_h^i} (\vartheta_E^i)^2 + \sum_{E \in \mathcal{E}_h^\partial} (\vartheta_E^\partial)^2.$$

Theorem 2.3. (A posteriori error estimate) Let Ψ be a regular solution of (2.1) and Ψ_h solve (2.4). For a sufficiently large penalty parameter $\sigma > 0$ and a sufficiently small discretization parameter h , there exists h -independent positive constants C_{rel} and C_{eff} such that

$$C_{eff}\vartheta \leq \|\Psi - \Psi_h\|_h \leq C_{rel}(\vartheta + h.o.t),$$

where $h.o.t$ expresses one or several terms of higher order (as will be explained in Section 4).

3 A priori error estimate

This section is devoted to the proof of Theorem 2.2. We present some auxiliary results first, followed by a discrete inf-sup condition and construct a non-linear map for the application of fixed point arguments. The energy and \mathbf{L}^2 - norm estimates follow as a consequence of the fixed point and duality arguments. The theoretical orders of convergence are confirmed by two numerical experiments.

3.1 Auxiliary results

Lemma 3.1. (Poincaré type inequalities)[10, 31, 34] Let Ω be a bounded open subset of \mathbb{R}^2 with Lipschitz continuous boundary $\partial\Omega$.

1. For $\varphi \in H_0^1(\Omega)$, there exists a positive constant $\alpha_0 = \alpha_0(\Omega)$ such that $\alpha_0\|\varphi\|_0 \leq \|\nabla\varphi\|_0$.
2. For $\varphi \in H^1(\mathcal{T})$, there exists a constant $C_P > 0$ independent of h and φ such that for $1 \leq r < \infty$, $\|\varphi\|_{L^r(\Omega)} \leq C_P\|\varphi\|_h$.

Lemma 3.2. (Discrete trace inequality) [6] For all $\Phi_h \in \mathbf{X}_h$, it holds that

$$\sum_{E \in \mathcal{E}_h^\partial} h_E \|\nabla\Phi_h \nu\|_{0,E}^2 \lesssim \|\nabla\Phi_h\|_0^2,$$

where the positive constant suppressed in " \lesssim " is independent of h .

Lemma 3.3. (Continuous trace inequality)[20] For $v \in H^1(T)$, $T \in \mathcal{T}$, it holds that

$$\|v\|_{0,\partial T}^2 \lesssim (h_T^{-1}\|v\|_{0,T}^2 + \|v\|_{0,T}\|\nabla v\|_{0,T}),$$

where the hidden constant in " \lesssim " is independent of h .

Lemma 3.4. (Interpolation estimate)[16, 22] For $v \in H^{1+\alpha}(\Omega)$ with $\alpha \in (0, 1]$, there exists $I_h v \in X_h$ such that

$$\|v - I_h v\|_0 + h\|v - I_h v\|_1 \leq C_I h^{1+\alpha} |v|_{H^{1+\alpha}(\Omega)},$$

where C_I is a positive constant independent of h .

Remark 3.5. A use of trace inequality in Lemma 3.3 yields $\|v - I_h v\|_h \leq C_I h^\alpha |v|_{H^{1+\alpha}(\Omega)}$ with some positive constant C_I independent of h .

Lemma 3.6. (Extension operator)[10, 29, 38] Define the operator $\Pi_h : X_h \rightarrow V_h := X_h \cap H_0^1(\Omega)$ using nodal values of freedom:

$$\begin{cases} \Pi_h v(n) = 0 & \text{for a node } n \text{ on } \partial\Omega, \\ \Pi_h v(n) = v(n) & \text{for a node } n \text{ on } \Omega \setminus \partial\Omega. \end{cases}$$

It holds that for all $v \in X_h$,

$$\left(\sum_{T \in \mathcal{T}_h} h_T^{-2} \|v - \Pi_h v\|_{0,T}^2 + \sum_{E \in \mathcal{E}_h^i} h_E^{-1} \|v - \Pi_h v\|_{0,E}^2 \right)^{\frac{1}{2}} \leq C_{e_1} \|v\|_h, \quad (3.1)$$

$$\|\nabla(v - \Pi_h v)\|_h \leq C_{e_2} \left(\sum_{E \in \mathcal{E}_h^\partial} \int_E h_E^{-1} v^2 ds \right)^{\frac{1}{2}} \leq C_{e_2} \|v\|_h, \quad \|\Pi_h v\|_h \leq C_{e_3} \|v\|_h, \quad (3.2)$$

where the constants C_{e_1} , C_{e_2} and C_{e_3} are independent of h .

The next lemma states boundedness and coercivity results for $A(\cdot, \cdot)$, boundedness results for $C(\cdot, \cdot)$ and $B(\cdot, \cdot, \cdot, \cdot)$ and for the corresponding discrete versions. These results are a consequence of Hölder's inequality, Lemma 3.1, and the Sobolev embedding results $H^1(\Omega) \hookrightarrow L^4(\Omega)$ and $H^{1+\alpha}(\Omega) \hookrightarrow L^\infty(\Omega)$ for $\Omega \subset \mathbb{R}^2$ and $\alpha > 0$. For detailed proofs, we refer to [39].

Lemma 3.7. (Boundedness and coercivity of continuous and discrete forms)[39, 43]

(i) For all $\Theta, \Phi \in \mathbf{V}$,

$$A(\Theta, \Phi) \leq \|\Theta\|_1 \|\Phi\|_1, \quad A(\Theta, \Theta) \geq \|\Theta\|_1^2, \quad (3.3)$$

$$\text{and } C(\Theta, \Phi) \lesssim \epsilon^{-2} \|\Theta\|_0 \|\Phi\|_0, \quad C_h(\Theta, \Phi) \lesssim \epsilon^{-2} \|\Theta\|_h \|\Phi\|_h. \quad (3.4)$$

(ii) For the choice of a sufficiently large parameter σ , there exists a positive constant $\alpha_1 > 0$ such that for $\Theta_h, \Phi_h \in \mathbf{X}_h$,

$$A_h(\Theta_h, \Phi_h) \leq \|\Theta_h\|_h \|\Phi_h\|_h, \quad \text{and } A_h(\Phi_h, \Phi_h) \geq \alpha_1 \|\Phi_h\|_h^2. \quad (3.5)$$

(iii) For $\Xi, \eta, \Theta, \Phi \in \mathbf{X}$, it holds that

$$\int_{\Omega} (\Xi \cdot \eta)(\Theta \cdot \Phi) dx \lesssim \|\Xi\|_1 \|\eta\|_1 \|\Theta\|_1 \|\Phi\|_1, \quad \sum_{T \in \mathcal{T}} \int_T (\Xi \cdot \eta)(\Theta \cdot \Phi) dx \lesssim \|\Xi\|_h \|\eta\|_h \|\Theta\|_h \|\Phi\|_h. \quad (3.6)$$

$$B(\Xi, \eta, \Theta, \Phi) \lesssim \epsilon^{-2} \|\Xi\|_1 \|\eta\|_1 \|\Theta\|_1 \|\Phi\|_1, \quad B_h(\Xi, \eta, \Theta, \Phi) \lesssim \epsilon^{-2} \|\Xi\|_h \|\eta\|_h \|\Theta\|_h \|\Phi\|_h \quad (3.7)$$

and for all $\Xi, \eta \in \mathbf{H}^{1+\alpha}(\Omega)$, $\Theta, \Phi \in \mathbf{X}$,

$$B_h(\Xi, \eta, \Theta, \Phi) \lesssim \epsilon^{-2} \|\Xi\|_{1+\alpha} \|\eta\|_{1+\alpha} \|\Theta\|_0 \|\Phi\|_0, \quad (3.8)$$

where the hidden constant in " \lesssim " depends on the constants from C_P, α_0 and C_S .

Some further properties of the quartic form $B_h(\cdot, \cdot, \cdot, \cdot)$ are stated in the next lemma. The proof is provided in Appendix A.1.

Lemma 3.8. (Properties of the quartic form)[39] (i) For $\eta \in \mathbf{X}$ and for all $\eta_h, \Phi_h \in \mathbf{X}_h$,

$$B_h(\eta_h, \eta_h, \eta_h, \Phi_h) - B_h(\eta, \eta, \eta, \Phi_h) \lesssim \epsilon^{-2} (\|\eta_h - \eta\|_h^2 \|\eta_h\|_h + \|\eta_h - \eta\|_h^2 \|\eta\|_1 + \|\eta_h - \eta\|_h \|\eta\|_1^2) \|\Phi_h\|_h.$$

(ii) For $\eta \in \mathbf{H}^{1+\alpha}(\Omega)$ with $\alpha > 0$ and $\eta_h = I_h \eta$,

$$B_h(I_h \eta, I_h \eta, I_h \eta, \Phi_h) - B_h(\eta, \eta, \eta, \Phi_h) \lesssim \epsilon^{-2} h^{2\alpha} \|\eta\|_{1+\alpha}^3 \|\Phi_h\|_h \text{ for all } \Phi_h \in \mathbf{X}_h.$$

(iii) For $\eta \in \mathbf{H}^{1+\alpha}(\Omega)$ with $\alpha > 0$, its interpolant $I_h \eta$ satisfies

$$B_h(\eta, \eta, \Theta_h, \Phi_h) - B_h(I_h \eta, I_h \eta, \Theta_h, \Phi_h) \lesssim \epsilon^{-2} h^\alpha \|\eta\|_{1+\alpha}^2 \|\Theta_h\|_h \|\Phi_h\|_h \text{ for all } \Theta_h, \Phi_h \in \mathbf{X}_h,$$

where the constants hidden in " \lesssim " are independent of h .

The following lemmas concern a few local efficiency type estimates that yield lower bounds for the errors, and are necessary for both the medius analysis and the efficiency estimates of the *a posteriori* error analysis. The proofs follow from standard bubble function techniques extended to the non-linear system considered in this paper and are given in Appendix A.3.

Lemma 3.9. (Local efficiency I) Let Ψ be a regular solution of (2.1) and $\Phi_h \in \mathbf{X}_h$. Set $\eta_T := (2\epsilon^{-2}(|\Phi_h|^2 - 1)\Phi_h)|_T$ defined on a triangle $T \in \mathcal{T}$ and $\eta_E := [\nabla \Phi_h \nu]_E$ on the edge E of T . Then the following estimates hold true.

$$(i) \sum_{T \in \mathcal{T}} h_T^2 \|\eta_T\|_{0,T}^2 + \sum_{E \in \mathcal{E}_h^i} h_E \|\eta_E\|_{0,E}^2 \lesssim \|\Psi - \Phi_h\|_h^2 (1 + \epsilon^{-2} (\|\Psi - \Phi_h\|_h (\|\Phi_h\|_1 + \|\Psi\|_1) + \|\Psi\|_1^2 + 1))^2. \quad (3.9)$$

(ii) For $\Phi_h = I_h \Psi$ with $\Psi \in \mathbf{H}^{1+\alpha}(\Omega)$, $\alpha > 0$,

$$\sum_{T \in \mathcal{T}} h_T^2 \|\eta_T\|_{0,T}^2 + \sum_{E \in \mathcal{E}_h^i} h_E \|\eta_E\|_{0,E}^2 \lesssim h^{2\alpha} (1 + \epsilon^{-2} h^\alpha (1 + \|\Psi\|_{1+\alpha}^2))^2 \|\Psi\|_{1+\alpha}^2.$$

We now discuss the well-posedness and regularity of solutions of a second-order linear system of equations (3.10) and a perturbation result that is important to prove the discrete inf-sup condition in the next section. The proof is given in Appendix A.2.

Lemma 3.10. (Linearized systems) *Let Ψ be a regular solution of (2.1). For a given $\Theta_h \in \mathbf{X}_h$ with $\|\Theta_h\|_h = 1$, there exist ξ and $\eta \in \mathbf{H}^{1+\alpha}(\Omega) \cap \mathbf{V}$ that solve the linear systems*

$$A(\xi, \Phi) = 3B_h(\Psi, \Psi, \Theta_h, \Phi) + C_h(\Theta_h, \Phi) \text{ for all } \Phi \in \mathbf{V} \text{ and} \quad (3.10)$$

$$A(\eta, \Phi) = 3B(\Psi, \Psi, \Pi_h \Theta_h, \Phi) + C(\Pi_h \Theta_h, \Phi) \text{ for all } \Phi \in \mathbf{V} \quad (3.11)$$

such that

$$\|\xi\|_{1+\alpha} \lesssim \epsilon^{-2}(1 + \|\Psi\|_{1+\alpha}^2) \quad \text{and} \quad \|\nabla(\eta - \xi)\|_0 \lesssim \epsilon^{-2}h(1 + \|\Psi\|_{1+\alpha}^2), \quad (3.12)$$

where the constant hidden in " \lesssim " depends on C_S , C_P and C_{e_1} .

The next lemma is a local efficiency type result for (3.10) that helps to prove the discrete inf-sup condition for a linear problem in the next section.

Lemma 3.11. (Local efficiency II) *Let ξ be the solution of (3.10) with interpolant $I_h \xi \in \mathbf{V}_h := \mathbf{X}_h \cap \mathbf{H}_0^1(\Omega)$. With the notations in Lemma 3.10, it holds that*

$$\sum_{T \in \mathcal{T}} h_T^2 \|\eta_T\|_{0,T}^2 + \sum_{E \in \mathcal{E}_h^i} h_E \|\eta_E\|_{0,E}^2 \lesssim \epsilon^{-4} h_T^{2\alpha} (1 + \|\Psi\|_{1+\alpha}^2)^2$$

where $\eta_T := (2\epsilon^{-2}(|I_h \Psi|^2 \Theta_h + 2(I_h \Psi \cdot \Theta_h)I_h \Psi - \Theta_h))|_T$ is defined on a triangle $T \in \mathcal{T}$, $I_h \Psi \in \mathbf{X}_h$ is the interpolant of Ψ and $\eta_E = [\nabla(I_h \xi)v]|_E$ on the edge E of T .

For $G \in \mathbf{L}^2(\Omega)$, the well-posed dual problem admits a unique $\chi \in \mathbf{V}$ [39] such that

$$\langle DN(\Psi)\Phi, \chi \rangle = (G, \Phi) \quad \text{for all } \Phi \in \mathbf{V}, \quad (3.13)$$

that satisfies

$$\|\chi\|_{1+\alpha} \lesssim (1 + \epsilon^{-2}(1 + \|\Psi\|_{1+\alpha}^2)) \|G\|_0, \quad (3.14)$$

where $\alpha \in (0, 1]$ denotes the index of elliptic regularity.

A local efficiency type result for (3.13) is useful for \mathbf{L}^2 - norm error estimates and is stated below.

Lemma 3.12. (Local efficiency III) *Let Ψ be a regular solution of (2.1) and $I_h \Psi \in \mathbf{X}_h$ be it's interpolant. For a given $G \in \mathbf{L}^2(\Omega)$, let χ solve (3.13) and let its interpolant be $I_h \chi \in \mathbf{V}_h$. Then, the following result holds.*

$$\sum_{T \in \mathcal{T}} h_T^2 \|\eta_T\|_{0,T}^2 + \sum_{E \in \mathcal{E}_h^i} h_E \|\eta_E\|_{0,E}^2 \lesssim h^{2\alpha} (1 + \epsilon^{-2}(1 + \|\Psi\|_{1+\alpha}^2))^4 \|G\|_0^2 + (Osc(G))^2,$$

where $\eta_T := (G - 2\epsilon^{-2}(|I_h \Psi|^2 I_h \chi + 2(I_h \Psi \cdot I_h \chi)I_h \Psi - I_h \chi))|_T$ is defined on a triangle $T \in \mathcal{T}$, $\eta_E := [\nabla(I_h \chi)v]|_E$ on edge E of T and

$$Osc(G) = \left(\sum_{T \in \mathcal{T}} h_T^2 \left(\inf_{G_h \in P_1(T)} \|G - G_h\|_{0,T}^2 \right) \right)^{\frac{1}{2}}.$$

Remark 3.13. In this article, we consider the case when exact solution belongs to $\mathbf{H}^{1+\alpha}(\Omega)$, $\alpha \in (0, 1]$. Hence globally continuous piece-wise affine polynomials in X_h lead to optimal order estimates. However, if the solution belongs to $\mathbf{H}^s(\Omega)$ for $\frac{3}{2} < s \leq p+1$, $p \in \mathbb{N}$, then we can choose $X_h = \{v_h \in C^0(\bar{\Omega}), v_h|_T \in P_p(T), \text{ for all } T \in \mathcal{T}\}$ [28]; in this case, the local efficiency terms $\eta_T := -\Delta \Phi_h + (2\epsilon^{-2}(|\Phi_h|^2 - 1)\Phi_h)|_T$ in Lemma 3.9. Similarly, η_T will include $\Delta(I_h \xi)$ and $\Delta(I_h \chi)$ in Lemmas 3.11 and 3.12, respectively.

3.2 Proof of *a priori* estimates

This subsection focuses on the *a priori* error estimates in Theorem 2.2. The key idea is to establish a discrete inf-sup condition that corresponds to a perturbed bilinear form defined for all $\Theta_h, \Phi_h \in \mathbf{X}_h$ as

$$\langle DN_h(I_h\Psi)\Theta_h, \Phi_h \rangle := A_h(\Theta_h, \Phi_h) + 3B_h(I_h\Psi, I_h\Psi, \Theta_h, \Phi_h) + C_h(\Theta_h, \Phi_h). \quad (3.15)$$

The proof of the discrete inf-sup condition in this article holds when the exact solution of (2.1) belongs to $\mathcal{X} \cap \mathbf{H}^{1+\alpha}(\Omega)$ with $\alpha \in (0, 1]$, whereas the proofs in [39, Theorem 4.7, Lemma 4.8] assume that the exact solution belongs to $\mathcal{X} \cap \mathbf{H}^2(\Omega)$. The non-trivial modification of the proof techniques appeal to a clever re-grouping of the terms that involve the boundary terms and an application of Lemma 3.11. The ideas of this proof can also be extended to improve the results in [39] when the exact solution is in $\mathcal{X} \cap \mathbf{H}^{1+\alpha}(\Omega)$.

Theorem 3.14. (Stability of perturbed bilinear form). *Let Ψ be a regular solution of (2.1) and $I_h\Psi$ be its interpolant from Lemma 3.4. For a sufficiently large σ and a sufficiently small discretization parameter h , there exists a constant β_0 such that (3.15) satisfies the following discrete inf-sup condition:*

$$0 < \beta_0 \leq \inf_{\substack{\Theta_h \in \mathbf{X}_h \\ \|\Theta_h\|_h = 1}} \sup_{\substack{\Phi_h \in \mathbf{X}_h \\ \|\Phi_h\|_h = 1}} \langle DN_h(I_h\Psi)\Theta_h, \Phi_h \rangle.$$

Proof. Let $\Theta_h \in \mathbf{X}_h$ with $\|\Theta_h\|_h = 1$ be given and let $I_h\xi$ be the interpolant of the solution ξ of (3.10). Since $\Theta_h + I_h\xi \in \mathbf{X}_h$, the discrete coercivity condition in (3.5) implies that there exists $\Phi_h \in \mathbf{X}_h$ with $\|\Phi_h\|_h = 1$ such that

$$\|\Theta_h + I_h\xi\|_h \lesssim A_h(\Theta_h + I_h\xi, \Phi_h).$$

Together with (3.10), (3.15) and a regrouping of terms, this yields

$$\begin{aligned} \|\Theta_h + I_h\xi\|_h \lesssim & \langle DN_h(I_h\Psi)\Theta_h, \Phi_h \rangle + (A_h(I_h\xi, \Phi_h) - A(\xi, \Pi_h\Phi_h)) + (3B_h(I_h\Psi, I_h\Psi, \Theta_h, \Pi_h\Phi_h - \Phi_h) \\ & + C_h(\Theta_h, \Pi_h\Phi_h - \Phi_h)) + 3(B_h(\Psi, \Psi, \Theta_h, \Pi_h\Phi_h) - B_h(I_h\Psi, I_h\Psi, \Theta_h, \Pi_h\Phi_h)). \end{aligned} \quad (3.16)$$

The definition of $A_h(\cdot, \cdot)$ leads to

$$\begin{aligned} A_h(I_h\xi, \Phi_h) - A(\xi, \Pi_h\Phi_h) &= (A(I_h\xi, \Phi_h - \Pi_h\Phi_h) - \langle \nabla(I_h\xi)v, \Phi_h \rangle_{\partial\Omega}) + A(I_h\xi - \xi, \Pi_h\Phi_h) \\ &\quad - \langle I_h\xi, \nabla\Phi_h v \rangle_{\partial\Omega} + \sum_{E \in \mathcal{E}_h^\partial} \frac{\sigma}{h_E} \langle I_h\xi, \Phi_h \rangle_E \\ &= (A(I_h\xi, \Phi_h - \Pi_h\Phi_h) - \langle \nabla(I_h\xi)v, \Phi_h \rangle_{\partial\Omega}) + A(I_h\xi - \xi, \Pi_h\Phi_h) \\ &\quad - \langle I_h\xi - \xi, \nabla\Phi_h v \rangle_{\partial\Omega} + \sum_{E \in \mathcal{E}_h^\partial} \frac{\sigma}{h_E} \langle I_h\xi - \xi, \Phi_h \rangle_E, \end{aligned} \quad (3.17)$$

where in the last step, we have used that $\xi = 0$ on $\partial\Omega$.

An integration by parts element-wise, and the facts that $\Delta(I_h\xi) = 0$, $\Pi_h\Phi_h = 0$ on $\partial\Omega$, $[\Phi_h - \Pi_h\Phi_h] = 0$ for all $E \in \mathcal{E}_h^i$ leads to an estimate for the first term in the right-hand side of (3.17) as

$$A(I_h\xi, \Phi_h - \Pi_h\Phi_h) - \langle \nabla(I_h\xi)v, \Phi_h - \Pi_h\Phi_h \rangle_{\partial\Omega} = \sum_{E \in \mathcal{E}_h^i} \langle [\nabla(I_h\xi)v], \Phi_h - \Pi_h\Phi_h \rangle_E.$$

Note that the above term can be combined with the third term on the right-hand side of (3.16) to rewrite the expression with the help of local term $\eta_T = (2\epsilon^{-2}(|I_h\Psi|^2\Theta_h + 2(I_h\Psi \cdot \Theta_h)I_h\Psi - \Theta_h))|_T$ on a triangle T and $\eta_E = [\nabla(I_h\xi)v]|_E$ on the edge E as

$$\begin{aligned} & A(I_h\xi, \Phi_h - \Pi_h\Phi_h) - \langle \nabla(I_h\xi)v, \Phi_h - \Pi_h\Phi_h \rangle_{\partial\Omega} + (3B_h(I_h\Psi, I_h\Psi, \Theta_h, \Pi_h\Phi_h - \Phi_h) + C_h(\Theta_h, \Pi_h\Phi_h - \Phi_h)) \\ &= - \sum_{T \in \mathcal{T}_h} \int_T \eta_T \cdot (\Phi_h - \Pi_h\Phi_h) \, dx + \sum_{E \in \mathcal{E}_h^i} \langle \eta_E, \Phi_h - \Pi_h\Phi_h \rangle_E. \end{aligned}$$

The Cauchy-Schwarz inequality, Lemma 3.11 and the inequality (3.1) applied to the right-hand side of the last equality yield

$$\begin{aligned}
& \sum_{T \in \mathcal{T}_h} \int_T \boldsymbol{\eta}_T \cdot (\Pi_h \Phi_h - \Phi_h) \, dx + \sum_{E \in \mathcal{E}_h^i} \langle \boldsymbol{\eta}_E, \Phi_h - \Pi_h \Phi_h \rangle_E \\
& \lesssim \left(\sum_{T \in \mathcal{T}_h} h_T^2 \|\boldsymbol{\eta}_T\|_{0,T}^2 \right)^{\frac{1}{2}} \left(\sum_{T \in \mathcal{T}_h} h_T^{-2} \|\Phi_h - \Pi_h \Phi_h\|_{0,T}^2 \right)^{\frac{1}{2}} + \left(\sum_{E \in \mathcal{E}_h^i} h_E \|\boldsymbol{\eta}_E\|_{0,E}^2 \right)^{\frac{1}{2}} \left(\sum_{E \in \mathcal{E}_h^i} h_E^{-1} \|\Phi_h - \Pi_h \Phi_h\|_{0,E}^2 \right)^{\frac{1}{2}} \\
& \lesssim \|\Phi_h\|_h \left(\sum_{T \in \mathcal{T}_h} h_T^2 \|\boldsymbol{\eta}_T\|_{0,T}^2 + \sum_{E \in \mathcal{E}_h^i} h_E \|\boldsymbol{\eta}_E\|_{0,E}^2 \right)^{\frac{1}{2}} \lesssim \epsilon^{-2} h^\alpha (1 + \|\Psi\|_{1+\alpha}^2). \tag{3.18}
\end{aligned}$$

Next we proceed to estimate the left over terms on the right-hand side of (3.17) and (3.16). These results are straightforward applications of the results in the last subsection. Lemma 3.7(i), Lemma 3.4, (3.2), $\|\Phi_h\|_h = 1$ and inequality (3.12) lead to

$$A(\mathbf{I}_h \boldsymbol{\xi} - \boldsymbol{\xi}, \Pi_h \Phi_h) \lesssim \|\nabla(\mathbf{I}_h \boldsymbol{\xi} - \boldsymbol{\xi})\|_0 \|\Phi_h\|_h \lesssim h^\alpha \|\boldsymbol{\xi}\|_{1+\alpha} \|\Phi_h\|_h \lesssim \epsilon^{-2} h^\alpha (1 + \|\Psi\|_{1+\alpha}^2). \tag{3.19}$$

The Cauchy-Schwarz inequality, Remark 3.5, Lemma 3.2, $\|\Phi_h\|_h = 1$ and (3.12) imply

$$\langle \mathbf{I}_h \boldsymbol{\xi} - \boldsymbol{\xi}, \nabla \Phi_h \nu \rangle_{\partial\Omega} \lesssim \|\mathbf{I}_h \boldsymbol{\xi} - \boldsymbol{\xi}\|_h \left(\sum_{E \in \mathcal{E}_h^\partial} h_E \|\nabla \Phi_h \nu\|_{0,E}^2 \right)^{\frac{1}{2}} \lesssim \epsilon^{-2} h^\alpha (1 + \|\Psi\|_{1+\alpha}^2). \tag{3.20}$$

$$\sum_{E \in \mathcal{E}_h^\partial} \frac{\sigma}{h_E} \langle \mathbf{I}_h \boldsymbol{\xi} - \boldsymbol{\xi}, \Phi_h \rangle_E \lesssim \|\mathbf{I}_h \boldsymbol{\xi} - \boldsymbol{\xi}\|_h \|\Phi_h\|_h \lesssim \epsilon^{-2} h^\alpha (1 + \|\Psi\|_{1+\alpha}^2). \tag{3.21}$$

Lemma 3.8(iii), (3.2), $\|\Theta_h\|_h = 1$ and $\|\Phi_h\|_h = 1$ lead to

$$3(B_h(\Psi, \Psi, \Theta_h, \Pi_h \Phi_h) - B_h(\mathbf{I}_h \Psi, \mathbf{I}_h \Psi, \Theta_h, \Pi_h \Phi_h)) \lesssim \epsilon^{-2} h^\alpha \|\Psi\|_{1+\alpha}^2. \tag{3.22}$$

A substitution of the estimates (3.18)- (3.22) in (3.16) leads to

$$\|\Theta_h + \mathbf{I}_h \boldsymbol{\xi}\|_h \lesssim \langle DN_h(\mathbf{I}_h \Psi) \Theta_h, \Phi_h \rangle + \epsilon^{-2} h^\alpha (1 + \|\Psi\|_{1+\alpha}^2). \tag{3.23}$$

The fact that Ψ is regular solution of (2.1) implies the inf-sup condition in (2.2). This with (3.11) and (3.3) implies that there exists $\Phi \in \mathbf{V}$ with $\|\Phi\|_1 = 1$ such that

$$\beta \|\Pi_h \Theta_h\|_1 \leq \langle DN(\Psi) \Pi_h \Theta_h, \Phi \rangle = A(\Pi_h \Theta_h + \boldsymbol{\eta}, \Phi) \leq \|\Pi_h \Theta_h + \boldsymbol{\eta}\|_h.$$

An introduction of intermediate terms and a triangle inequality lead to

$$\|\Pi_h \Theta_h + \boldsymbol{\eta}\|_h \lesssim \|\Pi_h \Theta_h - \Theta_h\|_h + \|\Theta_h + \mathbf{I}_h \boldsymbol{\xi}\|_h + \|\boldsymbol{\xi} - \mathbf{I}_h \boldsymbol{\xi}\|_h + \|\boldsymbol{\eta} - \boldsymbol{\xi}\|_1.$$

A triangle inequality followed by an application of the last two displayed inequalities yields

$$\begin{aligned}
1 = \|\Theta_h\|_h & \lesssim \|\Theta_h - \Pi_h \Theta_h\|_h + \|\Pi_h \Theta_h\|_1 \\
& \lesssim \|\Theta_h - \Pi_h \Theta_h\|_h + \|\Theta_h + \mathbf{I}_h \boldsymbol{\xi}\|_h + \|\mathbf{I}_h \boldsymbol{\xi} - \boldsymbol{\xi}\|_h + \|\boldsymbol{\xi} - \boldsymbol{\eta}\|_1. \tag{3.24}
\end{aligned}$$

Since $\boldsymbol{\xi} = 0$ on \mathcal{E}^∂ , (3.2) and a triangle inequality yield

$$\|\Theta_h - \Pi_h \Theta_h\|_h \leq C_{e_2} \left(\sum_{E \in \mathcal{E}^\partial} h_E^{-1} \|\Theta_h + \boldsymbol{\xi}\|_{0,E}^2 \right)^{\frac{1}{2}} \leq C_{e_2} \|\Theta_h + \boldsymbol{\xi}\|_h \leq C_{e_2} (\|\Theta_h + \mathbf{I}_h \boldsymbol{\xi}\|_h + \|\boldsymbol{\xi} - \mathbf{I}_h \boldsymbol{\xi}\|_h).$$

Use this in (3.24) and apply Lemma 3.4 and (3.12) to obtain

$$1 \lesssim \|\Theta_h + \mathbf{I}_h \boldsymbol{\xi}\|_h + \epsilon^{-2} h^\alpha (1 + \|\Psi\|_{1+\alpha}^2),$$

where the constant suppressed in ' \lesssim ' depends on $\alpha_0, C_S, C_P, C_I, C_{e_1}, C_{e_2}$, and C_{e_3} . Together with (3.23) this yields

$$1 \leq C_1 (\langle DN_h(\mathbf{I}_h \Psi) \Theta_h, \Phi_h \rangle + \epsilon^{-2} h^\alpha (1 + \|\Psi\|_{1+\alpha}^2)),$$

where the constant C_1 is independent of h . Therefore, for a given ϵ , the discrete inf-sup condition holds with $\beta_0 = \frac{1}{C_1}$ for $h < h_0 := \left(\frac{\epsilon^2}{2C_1(1 + \|\Psi\|_{1+\alpha}^2)} \right)^{\frac{1}{\alpha}}$. \square

Remark 3.15. In [39], under the assumption that exact solution has \mathbf{H}^2 regularity, the discrete inf-sup condition is established for a choice of $h = O(\epsilon^2)$. Though the $h - \epsilon$ dependency is not the focus of this paper, for the case $\alpha = 1$, where it is well-known[7] that $\|\Psi\|_2$ is bounded independent of ϵ , $h - \epsilon$ dependency results can be derived analogously as in [39].

Proof of energy norm estimate in Theorem 2.2. The proof is divided into four steps. In *Step 1*, a non-linear map $\mu_h : \mathbf{X}_h \rightarrow \mathbf{X}_h$ is constructed such that any fixed point of μ_h is a solution of the discrete non-linear problem (2.4). In *Step 2*, with help of Theorem 3.14, it is established that for a sufficiently large choice of the penalization parameter σ and a sufficiently small choice of discretization parameter h , there exists a positive constant $R(h)$ such that the well defined map μ_h maps the closed convex ball $\mathbb{B}_{R(h)}(\mathbf{I}_h\Psi)$ to itself. In *Step 3*, it is proved that the continuous mapping μ_h is a contraction. In *Step 4*, the existence of a unique fixed point of μ_h is proved using Brouwer's fixed point theorem, and the energy norm estimate is established.

Step 1 (Construction of μ_h): For $\Phi_h \in \mathbf{X}_h$, define the map $\mu_h : \mathbf{X}_h \rightarrow \mathbf{X}_h$ by

$$\langle DN_h(\mathbf{I}_h\Psi)\mu_h(\Theta_h), \Phi_h \rangle = 3B_h(\mathbf{I}_h\Psi, \mathbf{I}_h\Psi, \Theta_h, \Phi_h) - B_h(\Theta_h, \Theta_h, \Theta_h, \Phi_h) + L_h(\Phi_h) \quad (3.25)$$

and $\mathbb{B}_R(\mathbf{I}_h\Psi) := \{\Phi_h \in \mathbf{X}_h : \|\mathbf{I}_h\Psi - \Phi_h\|_h \leq R\}$. The map μ_h is well-defined, as follows from Theorem 3.14.

Step 2 (Mapping of ball to ball): In this step, we prove that

$$\|\Theta_h - \mathbf{I}_h\Psi\|_h \leq R(h) \implies \|\mu_h(\Theta_h) - \mathbf{I}_h\Psi\|_h \leq R(h) \text{ for all } \Theta_h \in \mathbf{X}_h.$$

The definition of $\langle DN_h(\mathbf{I}_h\Psi)\cdot, \cdot \rangle$ (3.25), followed by some simple algebra and a re-arrangement of terms leads to

$$\begin{aligned} \langle DN_h(\mathbf{I}_h\Psi)(\mathbf{I}_h\Psi - \mu_h(\Theta_h)), \Phi_h \rangle &= (A_h(\mathbf{I}_h\Psi, \Phi_h) + 3B_h(\mathbf{I}_h\Psi, \mathbf{I}_h\Psi, \mathbf{I}_h\Psi, \Phi_h) + C_h(\mathbf{I}_h\Psi, \Phi_h)) \\ &\quad - (3B_h(\mathbf{I}_h\Psi, \mathbf{I}_h\Psi, \Theta_h, \Phi_h) - B_h(\Theta_h, \Theta_h, \Theta_h, \Phi_h) + L_h(\Phi_h)) \\ &= (A_h(\mathbf{I}_h\Psi, \Phi_h - \Pi_h\Phi_h) - L_h(\Phi_h - \Pi_h\Phi_h)) + (C_h(\mathbf{I}_h\Psi, \Phi_h) + B_h(\mathbf{I}_h\Psi, \mathbf{I}_h\Psi, \mathbf{I}_h\Psi, \Phi_h)) \\ &\quad + (A_h(\mathbf{I}_h\Psi, \Pi_h\Phi_h) - L_h(\Pi_h\Phi_h)) + (2B_h(\mathbf{I}_h\Psi, \mathbf{I}_h\Psi, \mathbf{I}_h\Psi, \Phi_h) - 3B_h(\mathbf{I}_h\Psi, \mathbf{I}_h\Psi, \Theta_h, \Phi_h) \\ &\quad + B_h(\Theta_h, \Theta_h, \Theta_h, \Phi_h)). \end{aligned} \quad (3.26)$$

The definition of $A_h(\cdot, \cdot)$ and $L_h(\cdot)$, followed by an integration by parts element-wise for the term $A(\cdot, \cdot)$, $\Delta(\mathbf{I}_h\Psi) = 0$ and $[\Phi_h - \Pi_h\Phi_h] = 0$ for $E \in \mathcal{E}_h^i$ show that

$$\begin{aligned} A_h(\mathbf{I}_h\Psi, \Phi_h - \Pi_h\Phi_h) - L_h(\Phi_h - \Pi_h\Phi_h) &= \sum_{E \in \mathcal{E}_h^i} \langle [\nabla(\mathbf{I}_h\Psi)v], \Phi_h - \Pi_h\Phi_h \rangle_E + \langle \mathbf{g} - \mathbf{I}_h\Psi, \nabla(\Phi_h - \Pi_h\Phi_h)v \rangle_{\partial\Omega} \\ &\quad + \sum_{E \in \mathcal{E}_h^\partial} \frac{\sigma}{h_E} \langle \mathbf{I}_h\Psi - \mathbf{g}, \Phi_h - \Pi_h\Phi_h \rangle_E. \end{aligned} \quad (3.27)$$

Setting $\boldsymbol{\eta}_T = (2\epsilon^{-2}(|\mathbf{I}_h\Psi|^2 - 1)\mathbf{I}_h\Psi)|_T$ on a triangle T and $\boldsymbol{\eta}_E = [\nabla(\mathbf{I}_h\Psi)v]|_E$ on the edge E , the second term of (3.26) is estimated as

$$\begin{aligned} \sum_{E \in \mathcal{E}_h^i} \langle [\nabla(\mathbf{I}_h\Psi)v], \Phi_h - \Pi_h\Phi_h \rangle_E + C_h(\mathbf{I}_h\Psi, \Phi_h) + B_h(\mathbf{I}_h\Psi, \mathbf{I}_h\Psi, \mathbf{I}_h\Psi, \Phi_h) &= \left(\sum_{T \in \mathcal{T}_h} \int_T \boldsymbol{\eta}_T \cdot (\Phi_h - \Pi_h\Phi_h) dx \right. \\ &\quad \left. + \sum_{E \in \mathcal{E}_h^i} \langle \boldsymbol{\eta}_E, \Phi_h - \Pi_h\Phi_h \rangle_E \right) + (B_h(\mathbf{I}_h\Psi, \mathbf{I}_h\Psi, \mathbf{I}_h\Psi, \Pi_h\Phi_h) + C_h(\mathbf{I}_h\Psi, \Pi_h\Phi_h)). \end{aligned} \quad (3.28)$$

The definition of $A_h(\cdot, \cdot)$, the consistency of the exact solution Ψ given by $N_h(\Psi, \Pi_h\Phi_h) = L_h(\Pi_h\Phi_h)$ and $\Pi_h\Phi_h = 0$ on $\partial\Omega$ yields,

$$\begin{aligned} A_h(\mathbf{I}_h\Psi, \Pi_h\Phi_h) - L_h(\Pi_h\Phi_h) &= A(\mathbf{I}_h\Psi - \Psi, \Pi_h\Phi_h) + \langle \Psi - \mathbf{I}_h\Psi, \nabla(\Pi_h\Phi_h)v \rangle_{\partial\Omega} \\ &\quad - (B(\Psi, \Psi, \Psi, \Pi_h\Phi_h) + C(\Psi, \Pi_h\Phi_h)). \end{aligned} \quad (3.29)$$

A substitution of (3.27)-(3.29) in (3.26), a cancellation of a boundary term and suitable re-arrangement of terms leads to

$$\begin{aligned}
\langle DN_h(\mathbf{I}_h \Psi)(\mathbf{I}_h \Psi - \mu_h(\Theta_h)), \Phi_h \rangle &= \sum_{T \in \mathcal{T}_h} \int_T \boldsymbol{\eta}_T \cdot (\Phi_h - \Pi_h \Phi_h) \, dx + \sum_{E \in \mathcal{E}_h^i} \langle \boldsymbol{\eta}_E, (\Phi_h - \Pi_h \Phi_h) \rangle_E \\
&+ A(\mathbf{I}_h \Psi - \Psi, \Pi_h \Phi_h) + C(\mathbf{I}_h \Psi - \Psi, \Pi_h \Phi_h) + \langle \Psi - \mathbf{I}_h \Psi, \nabla \Phi_h \nu \rangle_{\partial \Omega} + \sum_{E \in \mathcal{E}_h^\partial} \frac{\sigma}{h_E} \langle \mathbf{I}_h \Psi - \mathbf{g}, \Phi_h - \Pi_h \Phi_h \rangle_E \\
&+ (B_h(\mathbf{I}_h \Psi, \mathbf{I}_h \Psi, \mathbf{I}_h \Psi, \Pi_h \Phi_h) - B(\Psi, \Psi, \Psi, \Pi_h \Phi_h)) + (2B_h(\mathbf{I}_h \Psi, \mathbf{I}_h \Psi, \mathbf{I}_h \Psi, \Phi_h) - 3B_h(\mathbf{I}_h \Psi, \mathbf{I}_h \Psi, \Theta_h, \Phi_h) \\
&+ B_h(\Theta_h, \Theta_h, \Theta_h, \Phi_h)). \tag{3.30}
\end{aligned}$$

Now we estimate the terms on the right-hand side of (3.30). A Cauchy-Schwarz inequality and Lemma 3.9(ii) leads to

$$\begin{aligned}
&\sum_{T \in \mathcal{T}_h} \int_T \boldsymbol{\eta}_T \cdot (\Phi_h - \Pi_h \Phi_h) \, dx + \sum_{E \in \mathcal{E}_h^i} \langle \boldsymbol{\eta}_E, (\Phi_h - \Pi_h \Phi_h) \rangle_E \\
&\lesssim \left(\sum_{T \in \mathcal{T}_h} h_T^2 \|\boldsymbol{\eta}_T\|_0^2 + \sum_{E \in \mathcal{E}_h^i} h_E \|\boldsymbol{\eta}_E\|_0^2 \right)^{\frac{1}{2}} \left(\sum_{T \in \mathcal{T}_h} h_T^{-2} \|\Phi_h - \Pi_h \Phi_h\|_{0,T}^2 + \sum_{E \in \mathcal{E}_h^i} h_E^{-1} \|\Phi_h - \Pi_h \Phi_h\|_{0,E}^2 \right)^{\frac{1}{2}} \\
&\lesssim h^\alpha (1 + \epsilon^{-2} h^\alpha (1 + \|\Psi\|_{1+\alpha}^2)) \|\Psi\|_{1+\alpha} \|\Phi_h\|_h, \tag{3.31}
\end{aligned}$$

where (3.1) is utilized in the last step. The following four estimates are obtained using Cauchy-Schwarz inequality, the definition of $\|\cdot\|_h$, Lemma 3.4, Remark 3.5, (3.2) and Lemma 3.2

$$A(\mathbf{I}_h \Psi - \Psi, \Pi_h \Phi_h) \lesssim \|\mathbf{I}_h \Psi - \Psi\|_h \|\Pi_h \Phi_h\|_h \lesssim h^\alpha \|\Psi\|_{1+\alpha} \|\Phi_h\|_h \tag{3.32}$$

$$C(\mathbf{I}_h \Psi - \Psi, \Pi_h \Phi_h) \lesssim \epsilon^{-2} \|\mathbf{I}_h \Psi - \Psi\|_0 \|\Phi_h\|_h \lesssim \epsilon^{-2} h^{1+\alpha} \|\Psi\|_{1+\alpha} \|\Phi_h\|_h \tag{3.33}$$

$$\begin{aligned}
\langle \Psi - \mathbf{I}_h \Psi, \nabla \Phi_h \nu \rangle_{\partial \Omega} &\leq \left(\sum_{E \in \mathcal{E}_h^\partial} \frac{\sigma}{h_E} \|\mathbf{I}_h \Psi - \Psi\|_{0,E}^2 \right)^{\frac{1}{2}} \left(\sum_{E \in \mathcal{E}_h^\partial} \frac{h_E}{\sigma} \|\nabla \Phi_h \nu\|_{0,E}^2 \right)^{\frac{1}{2}} \\
&\lesssim \|\mathbf{I}_h \Psi - \Psi\|_h \|\Phi_h\|_h \lesssim h^\alpha \|\Psi\|_{1+\alpha} \|\Phi_h\|_h \tag{3.34}
\end{aligned}$$

$$\begin{aligned}
\sum_{E \in \mathcal{E}_h^\partial} \frac{\sigma}{h_E} \langle \mathbf{I}_h \Psi - \mathbf{g}, \Phi_h - \Pi_h \Phi_h \rangle_E &\leq \left(\sum_{E \in \mathcal{E}_h^\partial} \frac{\sigma}{h_E} \|\mathbf{I}_h \Psi - \mathbf{g}\|_{0,E}^2 \right)^{\frac{1}{2}} \left(\sum_{E \in \mathcal{E}_h^\partial} \frac{\sigma}{h_E} \|\Phi_h - \Pi_h \Phi_h\|_{0,E}^2 \right)^{\frac{1}{2}} \\
&\leq \|\mathbf{I}_h \Psi - \Psi\|_h \|\Phi_h - \Pi_h \Phi_h\|_h \lesssim h^\alpha \|\Psi\|_{1+\alpha} \|\Phi_h\|_h, \tag{3.35}
\end{aligned}$$

where (3.5) (resp. (3.4)) are used in the first and second inequalities. Lemma 3.8(ii) and (3.2) yield

$$B_h(\mathbf{I}_h \Psi, \mathbf{I}_h \Psi, \mathbf{I}_h \Psi, \Pi_h \Phi_h) - B(\Psi, \Psi, \Psi, \Pi_h \Phi_h) \lesssim \epsilon^{-2} h^{2\alpha} \|\Psi\|_{1+\alpha}^3 \|\Phi_h\|_h. \tag{3.36}$$

The last term in the right-hand side of (3.30) is estimated similar to [39, T_4 in Theorem 5.1] and is presented here for the sake of continuity and clarity. Set $\tilde{\mathbf{e}} = \Theta_h - \mathbf{I}_h \Psi$ and use the definition of $B(\cdot, \cdot, \cdot, \cdot)$. Applications of the Cauchy-Schwarz inequality and relatively straightforward algebraic manipulations yield

$$\begin{aligned}
&2B_h(\mathbf{I}_h \Psi, \mathbf{I}_h \Psi, \mathbf{I}_h \Psi, \Phi_h) - 3B_h(\mathbf{I}_h \Psi, \mathbf{I}_h \Psi, \Theta_h, \Phi_h) + B_h(\Theta_h, \Theta_h, \Theta_h, \Phi_h) \\
&= 2\epsilon^{-2} \sum_{T \in \mathcal{T}} \int_T (|\Theta_h|^2 - |\mathbf{I}_h \Psi|^2)(\Theta_h \cdot \Phi_h) + 2(\mathbf{I}_h \Psi - \Theta_h) \cdot \mathbf{I}_h \Psi (\mathbf{I}_h \Psi \cdot \Phi_h) \, dx \\
&= 2\epsilon^{-2} \sum_{T \in \mathcal{T}} \int_T (\tilde{\mathbf{e}} \cdot (\tilde{\mathbf{e}} + 2\mathbf{I}_h \Psi)(\tilde{\mathbf{e}} + \mathbf{I}_h \Psi) \cdot \Phi_h - 2(\tilde{\mathbf{e}} \cdot \mathbf{I}_h \Psi)(\mathbf{I}_h \Psi \cdot \Phi_h)) \, dx \\
&= \epsilon^{-2} \sum_{T \in \mathcal{T}} \int_T ((\tilde{\mathbf{e}} \cdot \tilde{\mathbf{e}})(\tilde{\mathbf{e}} \cdot \Phi_h) + 2(\tilde{\mathbf{e}} \cdot \mathbf{I}_h \Psi)(\tilde{\mathbf{e}} \cdot \Phi_h) + (\tilde{\mathbf{e}} \cdot \tilde{\mathbf{e}})(\mathbf{I}_h \Psi \cdot \Phi_h)) \, dx \\
&\lesssim 2\epsilon^{-2} \|\tilde{\mathbf{e}}\|_h^2 (\|\tilde{\mathbf{e}}\|_h + \|\Psi\|_{1+\alpha}) \|\Phi_h\|_h. \tag{3.37}
\end{aligned}$$

A use of the discrete inf-sup condition in Lemma 3.14 yields that there exists a $\Phi_h \in \mathbf{X}_h$ with $\|\Phi_h\|_h = 1$ such that

$$\beta_0 \|\mathbf{I}_h \Psi - \mu_h(\Theta_h)\|_h \leq \langle DN_h(\mathbf{I}_h \Psi)(\mathbf{I}_h \Psi - \mu_h(\Theta_h)), \Phi_h \rangle. \quad (3.38)$$

A combination of the estimates in (3.31)- (3.37) and (3.38) with $\|\Phi_h\|_h = 1$ leads to

$$\|\mathbf{I}_h \Psi - \mu_h(\Theta_h)\|_h \lesssim h^\alpha (1 + \epsilon^{-2} h^\alpha (1 + \|\Psi\|_{1+\alpha}^2)) \|\Psi\|_{1+\alpha} + \epsilon^{-2} \|\tilde{\mathbf{e}}\|_h^2 (\|\tilde{\mathbf{e}}\|_h + \|\Psi\|_{1+\alpha}). \quad (3.39)$$

For a fixed value of ϵ , we have

$$\|\mathbf{I}_h \Psi - \mu_h(\Theta_h)\|_h \lesssim h^\alpha (1 + h^\alpha) + \|\tilde{\mathbf{e}}\|_h^2 (\|\tilde{\mathbf{e}}\|_h + 1).$$

Since $\Theta_h \in \mathbb{B}_R(\mathbf{I}_h \Psi)$, $\|\tilde{\mathbf{e}}\|_h = \|\Theta_h - \mathbf{I}_h \Psi\|_h \leq R(h)$. Therefore,

$$\|\mathbf{I}_h \Psi - \mu_h(\Theta_h)\|_h \leq C_2 (h^\alpha (1 + h^\alpha) + R(h)^2 (R(h) + 1)),$$

where C_2 is a constant independent of h . Choose $R(h) := 2C_2 h^\alpha$ and this yields

$$\|\mathbf{I}_h \Psi - \mu_h(\Theta_h)\|_h \leq C_2 h^\alpha (1 + h^\alpha (1 + 4C_2^2 (2C_2 h^\alpha + 1))).$$

For $h < h_2 := \min(h_0, h_1)$ with $h_1^\alpha < \frac{1}{1+4C_2^2(2C_2 h_0^\alpha + 1)}$, $\|\mathbf{I}_h \Psi - \mu_h(\Theta_h)\|_h \leq 2C_2 h^\alpha = R(h)$. This completes the proof of Step 2.

Step 3 (Contraction result): We establish that for all $\Theta_1, \Theta_2 \in \mathbb{B}_{R(h)}(\mathbf{I}_h \Psi)$, $\|\mu_h(\Theta_1) - \mu_h(\Theta_2)\|_h \lesssim h^\alpha (h^\alpha + 1) \|\Theta_1 - \Theta_2\|_h$. The proof follows the ideas of [39, Lemma 5.3] and a sketch is provided. For Θ_1 and $\Theta_2 \in \mathbb{B}_{R(h)}(\mathbf{I}_h \Psi)$, $\Phi_h \in \mathbf{X}_h$ with $\|\Phi_h\|_h = 1$, $\tilde{\mathbf{e}}_1 = \mathbf{I}_h \Psi - \Theta_1$, $\tilde{\mathbf{e}}_2 = \mathbf{I}_h \Psi - \Theta_2$, $\mathbf{e} = \Theta_1 - \Theta_2$, the definition of DN_h ; a regrouping of terms and boundedness results leads to

$$\begin{aligned} \|\mu_h(\Theta_1) - \mu_h(\Theta_2)\|_h &\leq \beta_0^{-1} \langle DN_h(\mathbf{I}_h \Psi)(\mu_h(\Theta_1) - \mu_h(\Theta_2)), \Phi_h \rangle \\ &\lesssim (\|\tilde{\mathbf{e}}_2\|_h + \|\tilde{\mathbf{e}}_1\|_h + \|\tilde{\mathbf{e}}_1\|_h^2 + \|\tilde{\mathbf{e}}_2\|_h^2) \|\mathbf{e}\|_h \|\Phi_h\|_h. \end{aligned}$$

A use of $\|\tilde{\mathbf{e}}_1\|_h, \|\tilde{\mathbf{e}}_2\|_h \leq 2C_2 h^\alpha$ yields $\|\mu_h(\Theta_1) - \mu_h(\Theta_2)\|_h \lesssim h^\alpha (h^\alpha + 1) \|\mathbf{e}\|_h$.

Step 4 (Existence, uniqueness and energy norm estimate): The map μ_h is well-defined follows as an application of Theorem 3.14. Steps 2 and 3 show that the nonlinear map μ_h is continuous and maps a closed convex subset $\mathbb{B}_R(\mathbf{I}_h \Psi)$ of a Hilbert space \mathbf{X}_h to itself. Therefore, the existence and uniqueness of the fixed point, say Ψ_h in the ball $\mathbb{B}_R(\mathbf{I}_h \Psi)$ follows from Brouwer's fixed point theorem [31] and Step 3. An application of the triangle inequality, the inequality $\|\mathbf{I}_h \Psi - \Psi_h\|_h \lesssim h^\alpha$ and Remark 3.5 yield the *a priori* error estimate in energy norm. \square

Remark 3.16. The proof of the energy norm estimate relies on the techniques of medius analysis [26] to deal with the milder regularity of the exact solution. This involves a different strategy for the proof using the local efficiency results in Step 2 when compared to [39, Theorem 5.1], where $\mathbf{H}^2(\Omega)$ regularity is assumed for the exact solution.

Remark 3.17. For $\alpha = 1$, that is, $\Psi \in \mathbf{H}^2(\Omega)$, it is well-known [7] that $\|\Psi\|_2$ is bounded independent of ϵ . In this case,

$$\|\mathbf{I}_h \Psi - \mu_h(\Theta_h)\|_h \leq C_3 (h(1 + \epsilon^{-2} h) + \epsilon^{-2} \|\tilde{\mathbf{e}}\|_h^2 (\|\tilde{\mathbf{e}}\|_h + 1)),$$

where the constant C_3 is independent of h and ϵ . For a sufficiently small choice of the discretization parameter chosen as $h = O(\epsilon^{2+\tau})$, $\tau > 0$ and $R(h) = 2C_3 h$, Steps 2, 3 hold. The modification of the proof in above theorem follows analogously to Theorem 5.1 in [39] and yields h - ϵ dependent estimates for this case.

Next, the L^2 norm error estimate is derived using the Aubin-Nitsche [16] duality technique. The proof relies on energy norm error bounds that has been established for a fixed ϵ . However, when $\Psi \in \mathbf{H}^2(\Omega)$, the proof can be modified as in Theorem 3.5 in [39] to obtain h - ϵ dependent estimates.

Proof of L^2 estimate in Theorem 2.2. Set $\varphi_h = I_h\Psi - \Psi_h$ and choose $G = \varphi_h$, $\Phi = \Pi_h\varphi_h$ in the continuous dual linear problem (3.13) to deduce

$$\|\varphi_h\|_0^2 = (\varphi_h, \varphi_h) = (\varphi_h, \varphi_h - \Pi_h\varphi_h) + \langle DN(\Psi)\Pi_h\varphi_h, \chi \rangle. \quad (3.40)$$

Let $I_h\chi \in V_h \subset \mathbf{H}_0^1(\Omega)$ denotes the interpolant of χ . A use of $I_h\chi = 0$ on $\partial\Omega$ implies

$$\langle DN(\Psi)\varphi_h, I_h\chi \rangle = \langle DN_h(\Psi)\varphi_h, I_h\chi \rangle + \langle \varphi_h, \nabla(I_h\chi)\nu \rangle_{\partial\Omega}.$$

Add and subtract $\langle DN(\Psi)(\varphi_h - \Pi_h\varphi_h), I_h\chi \rangle$ in the right hand side of (3.40), use the definition of $\langle DN(\Psi), \cdot \rangle$ and the last displayed identity with $\Pi_h\varphi_h = 0$ on $\partial\Omega$, and re-arrange the terms to obtain

$$\begin{aligned} \|\varphi_h\|_0^2 &= (\varphi_h, \varphi_h - \Pi_h\varphi_h) + (-A(I_h\chi, \varphi_h - \Pi_h\varphi_h) + \langle \nabla(I_h\chi)\nu, \varphi_h - \Pi_h\varphi_h \rangle_{\partial\Omega}) + (C(I_h\chi, \Pi_h\varphi_h - \varphi_h) \\ &\quad + 3B(\Psi, \Psi, I_h\chi, \Pi_h\varphi_h - \varphi_h)) + \langle DN(\Psi)\Pi_h\varphi_h, \chi - I_h\chi \rangle + \langle DN_h(\Psi)\varphi_h, I_h\chi \rangle \\ &=: T_1 + T_2 + T_3 + T_4 + T_5. \end{aligned} \quad (3.41)$$

A use of Hölder's inequality, (3.1) and the estimate $\|\varphi_h\|_h = \|\Psi - \Psi_h\|_h \lesssim h^\alpha$ from Step 2 of the proof of Theorem 2.2 leads to

$$T_1 = (\varphi_h, \varphi_h - \Pi_h\varphi_h) \leq \|\varphi_h - \Pi_h\varphi_h\|_0 \|\varphi_h\|_0 \lesssim h^{2\alpha} \|\varphi_h\|_0.$$

Apply integration by parts element-wise for the term $A(\varphi_h - \Pi_h\varphi_h, I_h\chi)$ in the expression of T_2 , use $\Delta(I_h\chi) = 0$ and recall the definitions of the local term $\eta_E = [\nabla(I_h\chi)\nu]_E$ on E from Lemma 3.12 with $G = \varphi_h$ and $Osc(\varphi_h) = 0$. This with a Cauchy-Schwarz inequality, Lemma 3.12, (3.1) and the estimate $\|\varphi_h\|_h \lesssim h^\alpha$ leads to

$$T_2 = -A(I_h\chi, \varphi_h - \Pi_h\varphi_h) + \langle \nabla(I_h\chi)\nu, \varphi_h - \Pi_h\varphi_h \rangle_{\partial\Omega} = \sum_{E \in \mathcal{E}_h^i} \langle \eta_E, \Pi_h\varphi_h - \varphi_h \rangle_E \lesssim h^{2\alpha} \|\varphi_h\|_0. \quad (3.42)$$

Lemma 3.7, (3.14), (3.2) and $\|\varphi_h\|_h \lesssim h^\alpha$ yield

$$T_3 = 3B(\Psi, \Psi, I_h\chi, \Pi_h\varphi_h - \varphi_h) + C(I_h\chi, \Pi_h\varphi_h - \varphi_h) \lesssim \|I_h\chi\|_h \|\Pi_h\varphi_h - \varphi_h\|_0 \lesssim h^{2\alpha} \|\varphi_h\|_0.$$

The boundedness and interpolation estimates in Lemmas 3.7, 3.4, (3.2) and $\|\varphi_h\|_h \lesssim h^\alpha$, and (3.14), leads to a bound for the fourth term of (3.41) as

$$T_4 = A(\Pi_h\varphi_h, \chi - I_h\chi) + 3B(\Psi, \Psi, \Pi_h\varphi_h, \chi - I_h\chi) + C(\Pi_h\varphi_h, \chi - I_h\chi) \lesssim h^{2\alpha} \|\chi\|_{1+\alpha} \lesssim h^{2\alpha} \|\varphi_h\|_0.$$

The discrete nonlinear problem (2.4) plus the consistency of the exact solution Ψ yield

$$N_h(\Psi, I_h\chi) = L_h(I_h\chi) = N_h(\Psi_h, I_h\chi).$$

Recall that $\varphi_h = I_h\Psi - \Psi_h$ and re-write the last term in (3.41) using the above displayed identity and the definitions of DN_h and N_h as

$$\begin{aligned} T_5 &= \langle DN_h(\Psi)\varphi_h, I_h\chi \rangle + N_h(\Psi_h, I_h\chi) - N_h(\Psi, I_h\chi) = A_h(I_h\Psi - \Psi, I_h\chi) + (C(I_h\Psi - \Psi, I_h\chi) \\ &\quad + 3B(\Psi, \Psi, I_h\Psi - \Psi, I_h\chi)) + (3B(\Psi, \Psi, \Psi - \Psi_h, I_h\chi) + B(\Psi_h, \Psi_h, \Psi_h, I_h\chi) - B(\Psi, \Psi, \Psi, I_h\chi)). \end{aligned}$$

An integration by parts element-wise for the $A(\Psi - I_h\Psi, I_h\chi)$ term, $\Delta I_h\chi = 0$, a Cauchy-Schwarz inequality, Lemma 3.12 with $G = \varphi_h$, $Osc(\varphi_h) = 0$ and Lemma 3.4 lead to an estimate for the first term on the right hand side of T_4 above as

$$\sum_{E \in \mathcal{E}_h^i} \langle \eta_E, I_h\Psi - \Psi \rangle_E \lesssim h^{2\alpha} \|\varphi_h\|_0. \quad (3.43)$$

Here, η_E is the local term as defined in the above estimates. Lemma 3.7, Remark 3.5 and (3.14) leads to an estimate for the second term in the expression on the right-hand side for T_5 above as

$$C(I_h\Psi - \Psi, I_h\chi) + 3B(\Psi, \Psi, \Psi - I_h\Psi, I_h\chi) \lesssim h^{2\alpha} \|\chi\|_{1+\alpha} \lesssim h^{2\alpha} \|\varphi_h\|_0. \quad (3.44)$$

To estimate the third term in the expression on the right-hand side for T_5 , modify the technique used in (3.37) and use Remark 3.5, (3.14) to obtain

$$\begin{aligned} & B(\Psi_h, \Psi_h, \Psi_h, I_h \chi) - B(\Psi, \Psi, \Psi, I_h \chi) + 3B(\Psi, \Psi, \Psi - \Psi_h, I_h \chi) \\ &= 2B(\Psi, \Psi, \Psi, I_h \chi) - 3B(\Psi, \Psi, \Psi_h, I_h \chi) + B(\Psi_h, \Psi_h, \Psi_h, I_h \chi) \\ &\lesssim \|\Psi - \Psi_h\|_h^2 (\|\Psi - \Psi_h\|_h + \|\Psi\|_1) \|I_h \chi\|_h \lesssim h^{2\alpha} \|\chi\|_{1+\alpha} \lesssim h^{2\alpha} \|\varphi_h\|_0. \end{aligned} \quad (3.45)$$

A combination of the estimates in (3.43)- (3.45) yields $T_5 \lesssim h^{2\alpha} \|\varphi_h\|_0$. Substitute the estimates derived for T_1, T_2, T_3, T_4 and T_5 in (3.41) and cancel the term $\|\varphi_h\|_0$ to obtain $\|I_h \Psi - \Psi_h\|_0 \lesssim h^{2\alpha}$. This estimate, a triangle inequality and Lemma 3.4 yield $\|\Psi - \Psi_h\|_0 \leq \|\Psi - I_h \Psi\|_0 + \|I_h \Psi - \Psi_h\|_0 \lesssim h^{2\alpha}$ and this concludes the proof. \square

3.3 Numerical results

In this section, we present a result on the quadratic convergence of Newton's method and some numerical examples that confirm the theoretical results obtained in the last section.

Preliminaries

- The uniform refinement process divides each triangle in the triangulation of the domain Ω into four similar triangles for subsequent mesh refinements.
- Let e_n and h_n (resp. e_{n-1} and h_{n-1}) denote the error and the discretization parameter at the n -th (resp. $n-1$ -th) level, respectively.
- The convergence rate at n -th level is defined by $\alpha_n := \log(e_n/e_{n-1})/\log(h_n/h_{n-1})$.
- The penalty parameter $\sigma = 10$ is chosen for all the numerical experiments.
- Newton's method is employed to compute the approximated solutions of the discrete nonlinear problem (2.4). The Newton's iterates Ψ_h^n , $n = 1, 2, \dots$ are

$$A_h(\Psi_h^n, \Phi_h) + 3B_h(\Psi_h^{n-1}, \Psi_h^{n-1}, \Psi_h^n, \Phi_h) + C_h(\Psi_h^n, \Phi_h) = 2B_h(\Psi_h^{n-1}, \Psi_h^{n-1}, \Psi_h^{n-1}, \Phi_h) + L_h(\Phi_h). \quad (3.46)$$

The proof of the quadratic convergence of the Newton iterates (3.46) to the discrete solution follows analogously to the proof of Theorem 3.6 in [39].

Theorem 3.18 (Convergence of Newton's method). *Let Ψ be a regular solution of the non-linear system (2.1) and let Ψ_h solve (2.4). For a choice of sufficiently large σ and sufficiently small discretization parameter, there exists $\rho_1 > 0$, independent of h , such that for any initial guess Ψ_h^0 with $\|\Psi_h^0 - \Psi_h\|_h \leq \rho_1$, it follows that $\|\Psi_h^n - \Psi_h\|_h \leq \frac{\rho_1}{2^n}$ for all $n = 1, 2, \dots$ and the iterates Ψ_h^n of Newton's method are well-defined and converge quadratically to Ψ_h ; that is, $\|\Psi_h^n - \Psi_h\|_h \leq C_q \|\Psi_h^{n-1} - \Psi_h\|_h^2$, where C_q is a constant independent of h .*

Example 3.1. (Square domain with benchmark example) Consider (2.1) on a convex domain $\Omega = (0, 1) \times (0, 1)$ with the Dirichlet boundary condition [37] given by

$$\mathbf{g} = \begin{cases} (T_d(x), 0) & \text{on } y = 0 \text{ and } y = 1, \\ (-T_d(y), 0) & \text{on } x = 0 \text{ and } x = 1, \end{cases}$$

where the parameter $d = 3\epsilon$ with $\epsilon = 0.02$ and the trapezoidal shape function $T_d : [0, 1] \rightarrow \mathbb{R}$ is defined by

$$T_d(t) = \begin{cases} t/d, & 0 \leq t \leq d, \\ 1, & d \leq t \leq 1-d, \\ (1-t)/d, & 1-d \leq t \leq 1. \end{cases} \quad (3.47)$$

We refer to [37, 39] for detailed construction of a suitable initial guess of Newton's iterates in this example. Tables 1 and 2 present the computed energy, error in energy and L^2 norms for numerical approximation of the diagonal D1 and rotated R1 solutions, respectively obtained using the Nitsche's method in (2.4). The orders of convergence agrees with the theoretical orders of convergence obtained in [37, 39, 45].

h	Energy	$\ \Psi_h^n - \Psi_h^{n-1}\ _h$	Order	$\ \Psi_h^n - \Psi_h^{n-1}\ _{L^2}$	Order
0.0220	79.24017828	1.84068650	-	0.92144678E-2	-
0.0110	78.29084590	1.01924858	0.85273798	0.29215012E-2	1.65719097
0.0055	78.03915719	0.53829987	0.92102395	0.88042589E-3	1.73043639
0.0027	77.97482243	0.27658883	0.96066718	0.23202911E-3	1.92389572

Table 1: Numerical energy, errors and convergence rates for D1 solution in energy and L^2 norms.

h	Energy	$\ \Psi_h^n - \Psi_h^{n-1}\ _h$	Order	$\ \Psi_h^n - \Psi_h^{n-1}\ _{L^2}$	Order
0.0220	87.90413862	1.86181020	-	0.95840689E-2	-
0.0110	86.93348566	1.02871941	0.85585647	0.29869842E-2	1.68194865
0.0055	86.67650908	0.54277993	0.92241024	0.89330907E-3	1.74145831
0.0027	86.61085704	0.27876870	0.96129876	0.23510836E-3	1.92583356

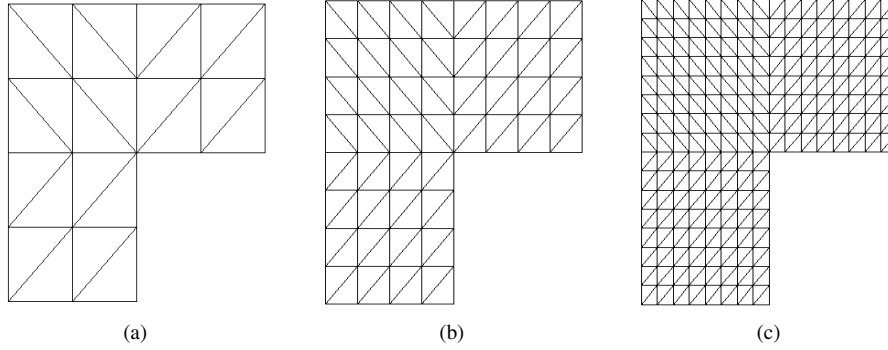
Table 2: Numerical energy, errors and convergence rates for R1 solution in energy and L^2 norms.

Figure 1: (a)Initial triangulation of L-shape domain and uniform refinements (b),(c).

Example 3.2. (*L*-shape domain with manufactured solution) In this example, consider (1.2) on a non-convex *L*-shape domain $\Omega = (-1, 1) \times (-1, 1) \setminus [0, 1] \times [-1, 0]$ with the parameter $\epsilon = 1$. For the manufactured solution $u = r^{2/3} \sin(2\theta/3)$, $v = r^{1/2} \sin(\theta/2)$, where (r, θ) denote the system of polar coordinates, compute the corresponding right hand side \mathbf{f} and the non-homogeneous Dirichlet boundary condition \mathbf{g} . In this case, the index of elliptic regularity is $\alpha \approx 0.5$ [25]. The discrete solution to (2.4) is obtained using the Newton's method defined in (3.46), with initial guess chosen as $\Psi_h^0 \in P_1(\mathcal{T})$ such that $A_h(\Psi_h^0, \Phi_h) = L_h(\Phi_h)$ for all $\Phi_h \in P_1(\mathcal{T})$, where $L_h(\cdot)$ is modified to contain the information about \mathbf{f} as well. Table 3 presents the convergence rates in energy norm and L^2 norm. The rates are of $O(h^\alpha)$ and $O(h^{2\alpha})$ as predicted in Theorem 2.2.

h	$\ \Psi - \Psi_h^n\ _h$	Order	$\ \Psi - \Psi_h^n\ _{L^2}$	Order
0.0883	0.21725459	-	0.13130447E-1	-
0.0441	0.15082475	0.52651342	0.57467070E-2	1.19210863
0.0220	0.10495374	0.52311952	0.25050066E-2	1.19792105
0.0110	0.07319673	0.51990257	0.10940019E-2	1.19519909
0.0055	0.05115870	0.51679942	0.47956567E-3	1.18981503
0.0027	0.03582649	0.51395282	0.21102915E-3	1.18428604

Table 3: Numerical errors and convergence rates in energy and L^2 norms for Example 3.2.

4 A posteriori error estimate

In this section, we first present some auxiliary results relevant for the *a posteriori* error estimates. The second subsection is devoted to the *a posteriori* error analysis for the Nitsche's method. The third subsection focuses on some numerical experiments and the performance of the adaptive algorithm. Note that, in this section, we assume that the non-homogeneous Dirichlet boundary condition $\mathbf{g} \in \mathbf{H}^{\frac{1}{2}}(\partial\Omega) \cap \mathbf{C}^0(\overline{\partial\Omega})$.

4.1 Auxiliary results

The approximation properties of the Scott-Zhang interpolation operator [22, 44] that are useful in this section are introduced first. This interpolation preserves the essential boundary condition on $\partial\Omega$.

Lemma 4.1. (*Scott-Zhang interpolation*) [22, 44] For $l, m \in \mathbb{N}$ with $1 \leq l < \infty$, there exists an interpolation operator $\mathbf{I}_h^{SZ} : H_0^l(\Omega) \rightarrow V_h := X_h \cap H_0^1(\Omega)$ that satisfies the stability and approximation properties given by: (a) for all $0 \leq m \leq \min(1, l)$, $\|\mathbf{I}_h^{SZ} v\|_{m,\Omega} \leq C_{SZ} \|v\|_{l,\Omega}$ for all $v \in H_0^l(\Omega)$, (b) provided $l \leq 2$, for all $0 \leq m \leq l$, $\|v - \mathbf{I}_h^{SZ} v\|_{m,T} \leq C_{SZ} h_T^{l-m} |v|_{l,\omega_T}$ for all $v \in H_0^l(\omega_T)$ and $T \in \mathcal{T}$, where the constant $C_{SZ} > 0$ is independent of h , and ω_T is the set of all triangles in \mathcal{T} that share at least one vertex with T .

Lemma 4.2. [32, Page 48] Let $\Psi_{\mathbf{g}} \in \mathcal{X}$ solve $\int_{\Omega} \nabla \Psi_{\mathbf{g}} \cdot \nabla \Phi \, dx = \sum_{T \in \mathcal{T}} \int_T \nabla \Psi_h \cdot \nabla \Phi \, dx$ for all $\Phi \in \mathbf{V}$, where Ψ_h is the solution of (2.4). Then there exists a constant $C > 0$, depending only on the minimum angle of \mathcal{T} such that $\sum_{T \in \mathcal{T}} \|\nabla(\Psi_{\mathbf{g}} - \Psi_h)\|_{0,T}^2 \leq C(\vartheta_{hot}^{\partial})^2$, where $(\vartheta_{hot}^{\partial})^2 := \sum_{E \in \mathcal{E}_h^{\partial}} h_E^{-1} \|\mathbf{g} - \mathbf{g}_h\|_{0,E}^2 + h_E \|\nabla(\mathbf{g} - \mathbf{g}_h)\|_{0,E}^2$,

\mathbf{g}_h being the standard Lagrange interpolant [16] of \mathbf{g} from $\mathbf{P}_2(\mathcal{E}_h^{\partial}) \cap \mathbf{C}^0(\overline{\partial\Omega})$.

Remark 4.3. Note that the benchmark liquid crystal example: Example 3.1 in [37] has Lipschitz continuous boundary conditions. Hence the *a posteriori* error analysis of this paper is applicable to this example and the results are illustrated in the section on Numerical experiments.

4.2 Proof of the *a posteriori* error estimate

The proof of Theorem 2.3, stated in Subsection 2.3, is presented in this section. An abstract estimate for the case of non-homogeneous boundary conditions and quartic nonlinearity is derived modifying the methodology in [15, 46] first and this result is crucial for the proof of Theorem 2.3.

Theorem 4.4. Let Ψ be a regular solution to (2.1) and $\Psi_{\mathbf{g}} \in \mathcal{X}$. Then, there exists a constant $R > 0$ such that for all $\boldsymbol{\eta}_h \in B(\Psi, R)$,

$$\|\Psi - \boldsymbol{\eta}_h\|_h \lesssim \|N(\boldsymbol{\eta}_h)\|_{\mathbf{V}^*} + (1 + \|DN(\boldsymbol{\eta}_h)\|_{\mathcal{L}(\mathbf{X}, \mathbf{V}^*)}) \|\Psi_{\mathbf{g}} - \boldsymbol{\eta}_h\|_h, \quad (4.1)$$

where the constant in " \lesssim " depends on γ in (4.2), continuous inf-sup constant β and Poincaré constant C_P , and the nonlinear (resp. linearized) operator $N(\cdot)$ (resp. $DN(\cdot)$) is defined in (2.1) (resp. (2.2)).

Proof. In the first step, we establish that for a given $R_0 > 0$, the operator DN restricted to $B(\Psi, R_0)$ is Lipschitz continuous and

$$\gamma := \sup_{\boldsymbol{\eta} \in B(\Psi, R_0)} \frac{\|DN(\boldsymbol{\eta}) - DN(\Psi)\|_{\mathcal{L}(\mathbf{X}, \mathbf{V}^*)}}{\|\boldsymbol{\eta} - \Psi\|_h} < \infty. \quad (4.2)$$

Here $\mathcal{L}(\mathbf{X}, \mathbf{V}^*)$ denotes the space of continuous linear maps from \mathbf{X} to \mathbf{V}^* . Let $R_0 > 0$ be given and $\boldsymbol{\eta} \in B(\Psi, R_0)$. For $\Theta \in \mathbf{X}$ and $\Phi \in \mathbf{V}$, the definition of $DN(\cdot)$, $B(\cdot, \cdot, \cdot, \cdot)$, a re-grouping of terms and (3.6) leads to

$$\begin{aligned} & \langle DN(\boldsymbol{\eta})\Theta, \Phi \rangle - \langle DN(\Psi)\Theta, \Phi \rangle = 3B(\boldsymbol{\eta}, \boldsymbol{\eta}, \Theta, \Phi) - 3B(\Psi, \Psi, \Theta, \Phi) \\ & = 2\epsilon^{-2} \int_{\Omega} ((\boldsymbol{\eta} - \Psi) \cdot (\boldsymbol{\eta} + \Psi)) (\Theta \cdot \Phi) + 2(\boldsymbol{\eta} - \Psi) \cdot \Theta (\boldsymbol{\eta} \cdot \Phi) + 2(\Psi \cdot \Theta) (\boldsymbol{\eta} - \Psi) \cdot \Phi \, dx \\ & \lesssim \epsilon^{-2} \|\boldsymbol{\eta} - \Psi\|_1 (R_0 + \|\Psi\|_1) \|\Theta\|_1 \|\Phi\|_1. \end{aligned} \quad (4.3)$$

The above displayed inequality with definition of $\|DN(\boldsymbol{\eta}) - DN(\Psi)\|_{\mathcal{L}(\mathbf{X}, \mathbf{V}^*)}$ leads to the Lipschitz continuity and this together with Lemma 3.1 concludes the proof of the first result.

Step two establishes (4.1). The continuous formulation (2.1) and a Taylor expansion lead to

$$0 = N(\Psi; \Phi) = N(\boldsymbol{\eta}_h; \Phi) + \left\langle \int_0^1 DN(\Psi + t(\boldsymbol{\eta}_h - \Psi))(\Psi - \boldsymbol{\eta}_h) dt, \Phi \right\rangle.$$

Introduce $\pm \langle DN(\Psi)(\Psi - \boldsymbol{\eta}_h), \Phi \rangle$ in the above displayed expression and rearrange the terms to obtain

$$\langle DN(\Psi)(\Psi - \boldsymbol{\eta}_h), \Phi \rangle = -N(\boldsymbol{\eta}_h; \Phi) - \left\langle \int_0^1 (DN(\Psi + t(\boldsymbol{\eta}_h - \Psi)) - DN(\Psi))(\Psi - \boldsymbol{\eta}_h) dt, \Phi \right\rangle. \quad (4.4)$$

Rewrite $\Psi - \boldsymbol{\eta}_h$ as $(\Psi - \Psi_{\mathbf{g}}) + (\Psi_{\mathbf{g}} - \boldsymbol{\eta}_h)$ in the left-hand side of the term above, use linearity of $\langle DN(\Psi), \cdot, \cdot \rangle$, introduce $\pm \langle DN(\boldsymbol{\eta}_h)(\Psi_{\mathbf{g}} - \boldsymbol{\eta}_h), \Phi \rangle$ in (4.4) in the first step; and bound in the second step to obtain

$$\begin{aligned} \langle DN(\Psi)(\Psi - \Psi_{\mathbf{g}}), \Phi \rangle &= -N(\boldsymbol{\eta}_h; \Phi) + \langle (DN(\boldsymbol{\eta}_h) - DN(\Psi))(\Psi_{\mathbf{g}} - \boldsymbol{\eta}_h), \Phi \rangle - \langle DN(\boldsymbol{\eta}_h)(\Psi_{\mathbf{g}} - \boldsymbol{\eta}_h), \Phi \rangle \\ &\quad - \left\langle \int_0^1 (DN(\Psi + t(\boldsymbol{\eta}_h - \Psi)) - DN(\Psi))(\Psi - \boldsymbol{\eta}_h) dt, \Phi \right\rangle \\ &\lesssim (\|N(\boldsymbol{\eta}_h)\|_{\mathbf{V}^*} + \|DN(\boldsymbol{\eta}_h) - DN(\Psi)\|_{\mathcal{L}(\mathbf{X}, \mathbf{V}^*)}) \|\Psi_{\mathbf{g}} - \boldsymbol{\eta}_h\|_1 + \|DN(\boldsymbol{\eta}_h)\|_{\mathcal{L}(\mathbf{X}, \mathbf{V}^*)} \|\Psi_{\mathbf{g}} - \boldsymbol{\eta}_h\|_1 \\ &\quad + \int_0^1 \| (DN(\Psi + t(\boldsymbol{\eta}_h - \Psi)) - DN(\Psi)) \|_{\mathcal{L}(\mathbf{X}, \mathbf{V}^*)} \|\Psi - \boldsymbol{\eta}_h\|_1 dt \|\Phi\|_1. \end{aligned} \quad (4.5)$$

Since $\Psi_{\mathbf{g}} \in \mathcal{X}$, $\Psi - \Psi_{\mathbf{g}} \in \mathbf{V}$. For $\delta > 0$ small enough, the continuous inf-sup condition (2.2) implies that there exists $\Phi \in \mathbf{V}$ with $\|\Phi\|_1 = 1$ such that

$$(\beta - \delta) \|\Psi - \Psi_{\mathbf{g}}\|_1 \leq \langle DN(\Psi)(\Psi - \Psi_{\mathbf{g}}), \Phi \rangle.$$

A triangle inequality, $\Psi - \Psi_{\mathbf{g}} = 0$ on $\partial\Omega$ and the last displayed inequality yield

$$(\beta - \delta) \|\Psi - \boldsymbol{\eta}_h\|_h \leq (\beta - \delta) (\|\Psi - \Psi_{\mathbf{g}}\|_1 + \|\Psi_{\mathbf{g}} - \boldsymbol{\eta}_h\|_h) \lesssim \langle DN(\Psi)(\Psi - \Psi_{\mathbf{g}}), \Phi \rangle + (\beta - \delta) \|\Psi_{\mathbf{g}} - \boldsymbol{\eta}_h\|_h.$$

Take $\delta \rightarrow 0$ to obtain

$$\beta \|\Psi - \boldsymbol{\eta}_h\|_h \lesssim \langle DN(\Psi)(\Psi - \Psi_{\mathbf{g}}), \Phi \rangle + \beta \|\Psi_{\mathbf{g}} - \boldsymbol{\eta}_h\|_h. \quad (4.6)$$

A combination of (4.5) and (4.6) together with (4.2), Poincaré type inequality in Lemma 3.1 for $\|\Phi\|_1 = 1$ leads to

$$C_4 \|\Psi - \boldsymbol{\eta}_h\|_h \leq \|N(\boldsymbol{\eta}_h)\|_{\mathbf{V}^*} + (1 + \|\Psi - \boldsymbol{\eta}_h\|_h + \|DN(\boldsymbol{\eta}_h)\|_{\mathcal{L}(\mathbf{X}, \mathbf{V}^*)}) \|\Psi_{\mathbf{g}} - \boldsymbol{\eta}_h\|_h + \|\Psi - \boldsymbol{\eta}_h\|_h^2,$$

where the constant C_4 depends on β , γ and C_P . For a choice of $R := \min\{R_0, C_4/2\}$, use $\|\Psi - \boldsymbol{\eta}_h\|_h < C_4/2$ and $\|\Psi - \boldsymbol{\eta}_h\|_h^2 < C_4/2 \|\Psi - \boldsymbol{\eta}_h\|_h$ in the second and third terms respectively, in the right hand side of the above inequality to obtain

$$C_4/2 \|\Psi - \boldsymbol{\eta}_h\|_h \leq \|N(\boldsymbol{\eta}_h)\|_{\mathbf{V}^*} + (1 + C_4/2 + \|DN(\boldsymbol{\eta}_h)\|_{\mathcal{L}(\mathbf{X}, \mathbf{V}^*)}) \|\Psi_{\mathbf{g}} - \boldsymbol{\eta}_h\|_h,$$

and this leads to the desired conclusion. \square

Next, the main result of this section is proven in the following text.

Proof of Theorem 2.3. Theorem 2.2 guarantees the existence of $R > 0$ such that (4.1) holds for a choice of $\boldsymbol{\eta}_h = \Psi_h$. Choose $\Psi_{\mathbf{g}}$ as in Lemma 4.2. A *posteriori* reliability (resp. efficiency) estimate provides an upper bound (resp. lower bound) on the discretization error, up to a constant.

To establish the reliability, Theorem 4.4 is utilized and the term $\|N(\Psi_h)\|_{\mathbf{V}^*}$ is estimated first. Since \mathbf{V} is a Hilbert space, there exists a $\Phi \in \mathbf{V}$ with $\|\Phi\|_1 = 1$ such that

$$\|N(\Psi_h)\|_{\mathbf{V}^*} = N(\Psi_h; \Phi) = N(\Psi_h; \Phi - \mathbf{I}_h^{SZ}\Phi) + N(\Psi_h; \mathbf{I}_h^{SZ}\Phi), \quad (4.7)$$

where $I_h^{SZ} : \mathbf{V} \rightarrow \mathbf{V}_h$ is the Scott-Zhang interpolation in Lemma 4.1. The second term in (4.7) can be rewritten using (2.4) with test function $I_h^{SZ}\Phi$ (that vanishes on $\partial\Omega$) as

$$\begin{aligned} N(\Psi_h; I_h^{SZ}\Phi) &= \langle \Psi_h - \mathbf{g}, \nabla(I_h^{SZ}\Phi)v \rangle_{\partial\Omega} \lesssim \left(\sum_{E \in \mathcal{E}_h^\partial} \frac{\sigma}{h_E} \|\Psi_h - \mathbf{g}\|_0^2 \right)^{\frac{1}{2}} \left(\sum_{E \in \mathcal{E}_h^\partial} \frac{h_E}{\sigma} \|\nabla(I_h^{SZ}\Phi)v\|_0^2 \right)^{\frac{1}{2}} \\ &\lesssim \left(\sum_{E \in \mathcal{E}_h^\partial} \frac{\sigma}{h_E} \|\Psi_h - \mathbf{g}\|_0^2 \right)^{\frac{1}{2}} = \left(\sum_{E \in \mathcal{E}_h^\partial} (\vartheta_E^\partial)^2 \right)^{1/2}, \end{aligned} \quad (4.8)$$

where for $\|\Phi\|_1 = 1$, a Cauchy-Schwarz inequality, Lemmas 3.2 and 4.1 are utilized in the second and third steps.

Apply integration by parts element-wise for $A(\Psi_h, \Phi - I_h^{SZ}\Phi)$ in the expression of $N(\Psi_h; \Phi - I_h^{SZ}\Phi)$, use $[\Phi - I_h^{SZ}\Phi] = 0$ on $E \in \mathcal{E}_h^i$, $\Phi - I_h^{SZ}\Phi = 0$ on $\partial\Omega$, $\Delta\Psi_h = 0$ and recall the definition of the local terms $\boldsymbol{\eta}_T := (2\epsilon^{-2}(|\Psi_h|^2 - 1)\Psi_h)|_T$ defined on a triangle $T \in \mathcal{T}$ and $\boldsymbol{\eta}_E := [\nabla\Psi_h v]|_E$ on the edge E of T . For $\|\Phi\|_1 = 1$, the above arguments, Cauchy-Schwarz inequality and Lemma 4.1 lead to

$$\begin{aligned} N(\Psi_h; \Phi - I_h^{SZ}\Phi) &= A(\Psi_h, \Phi - I_h^{SZ}\Phi) + B(\Psi_h, \Psi_h, \Psi_h, \Phi - I_h^{SZ}\Phi) + C(\Psi_h, \Phi - I_h^{SZ}\Phi) \\ &= \sum_{T \in \mathcal{T}_h} \int_T \boldsymbol{\eta}_T \cdot (\Phi - I_h^{SZ}\Phi) \, dx + \sum_{E \in \mathcal{E}_h^i} \langle \boldsymbol{\eta}_E, \Phi - I_h^{SZ}\Phi \rangle_E \\ &\lesssim \left(\sum_{T \in \mathcal{T}_h} \vartheta_T^2 + \sum_{E \in \mathcal{E}_h^i} (\vartheta_E^i)^2 \right)^{\frac{1}{2}} \left(\sum_{T \in \mathcal{T}_h} h_T^{-2} \|\Phi - I_h^{SZ}\Phi\|_{0,T}^2 + \sum_{E \in \mathcal{E}_h^i} h_E^{-1} \|\Phi - I_h^{SZ}\Phi\|_{0,E}^2 \right)^{\frac{1}{2}} \\ &\lesssim \left(\sum_{T \in \mathcal{T}_h} \vartheta_T^2 + \sum_{E \in \mathcal{E}_h^i} (\vartheta_E^i)^2 \right)^{\frac{1}{2}}, \end{aligned} \quad (4.9)$$

where $\vartheta_T^2 = h_T^2 \|(2\epsilon^{-2}(|\Psi_h|^2 - 1)\Psi_h)\|_{0,T}^2$, and $(\vartheta_E^i)^2 = h_E \|[\nabla\Psi_h v]\|_{0,E}^2$ for all $E \in \mathcal{E}_h^i$. A use of (4.8), (4.9) in (4.7) leads to the estimate of $\|N(\Psi_h)\|_{\mathbf{V}^*}$.

The second term in (4.1) is bounded using $\sum_{E \in \mathcal{E}_h^\partial} (\vartheta_E^\partial)^2$ in (2.6) and Lemma 4.2 by *higher order terms* (h.o.t.) [13] that consist of (i) the errors arising due to the polynomial approximation of the boundary data \mathbf{g} that depends on the given data smoothness and (ii) the terms $\|DN(\Psi_h)\|_{\mathcal{L}(\mathbf{X}, \mathbf{V}^*)} \|\Psi_{\mathbf{g}} - \Psi_h\|_h$.

The definition of $\|\cdot\|_h$ and Lemma 4.2 yield

$$\|\Psi_{\mathbf{g}} - \Psi_h\|_h^2 = \sum_{T \in \mathcal{T}} \|\nabla(\Psi_{\mathbf{g}} - \Psi_h)\|_{0,T}^2 + \sum_{E \in \mathcal{E}_h^\partial} \frac{\sigma}{h_E} \|\Psi_h - \mathbf{g}\|_{0,E}^2 \lesssim (\vartheta_{hot}^\partial)^2 + \sum_{E \in \mathcal{E}_h^\partial} (\vartheta_E^\partial)^2.$$

Set $\Phi_h = \Psi_h$ and $\boldsymbol{\eta}_T = (2\epsilon^{-2}(|\Psi_h|^2 - 1)\Psi_h)|_T$ on a triangle T and $\boldsymbol{\eta}_E = [\nabla\Psi_h v]|_E$ on a edge E in Lemma 3.9. A use of the local efficiency estimates in (3.9) and

$$\sum_{E \in \mathcal{E}^\partial} (\vartheta_E^\partial)^2 = \sum_{E \in \mathcal{E}^\partial} \frac{1}{h_E} \|\Psi_h - \mathbf{g}\|_{0,E}^2 \leq \|\Psi - \Psi_h\|_h^2$$

establishes the lower bound in Theorem 2.3. \square

Remark 4.5. For $X_h = \{v_h \in C^0(\overline{\Omega}), v_h|_T \in P_p(T), \text{ for all } T \in \mathcal{T}\}$, if we use higher order polynomials for the approximation, then $\vartheta_T^2 = h_T^2 \|\Delta\Psi_h + 2\epsilon^{-2}(|\Psi_h|^2 - 1)\Psi_h\|_{0,T}^2$ in (2.5).

4.3 Numerical results

This subsection focuses on some numerical experiments that illustrate the practical performances of the error indicators in adaptive mesh refinement for Nitsche's method.

Preliminaries

- The discrete solution to (2.4) is obtained using the Newton's method defined in (3.46) with initial guess $\Psi_h^0 \in P_1(\mathcal{T})$, as computed in the examples of Section 3.3 and mentioned otherwise.
- The penalty parameter is consistently chosen to be $\sigma = 10$ in all the numerical experiments.
- Let $e(l)$ and $\text{Ndof}(l)$ be the error and total number of unknowns at the l -th level refinement respectively. The convergence rates with respect to Ndof (in contrast to h in Section 3.3) are calculated as

$$\text{Order}_e(l) := \frac{\log(e(l-1)/e(l))}{\log(\text{Ndof}(l)/\text{Ndof}(l-1))} \quad \text{and} \quad \text{Order}_\vartheta(l) := \frac{\log(\vartheta(l-1)/\vartheta(l))}{\log(\text{Ndof}(l)/\text{Ndof}(l-1))}.$$

- Given an initial triangulation \mathcal{T}_0 , run the steps **SOLVE**, **ESTIMATE**, **MARK** and **REFINE** successively for different levels $l = 0, 1, 2, \dots$

SOLVE Compute the solution $\Psi_h = (u_h, v_h)$ of the discrete problem (2.4) for each triangulation.

ESTIMATE Calculate the error indicator $\Xi_{T,l}$ for each element $T \in \mathcal{T}_l$ given by

$$\Xi_{T,l}^2 := \vartheta_T^2 + \sum_{E \in \partial T \cap \mathcal{E}_h^i} (\vartheta_E^i)^2 + \sum_{E \in \partial T \cap \mathcal{E}_h^p} (\vartheta_E^p)^2.$$

MARK For next refinement, mark the elements $T \in \mathcal{T}_l$ such that

$$\Xi_{T,l} \geq \frac{1}{2} \max_{T \in \mathcal{T}_l} \Xi_{T,l}$$

and collect those elements to construct a subset $\tilde{\mathcal{T}} \subset \mathcal{T}_l$.

REFINE The subset $\tilde{\mathcal{T}}$ of marked elements will be refined using the marked edge bisection [46] refinement strategy to construct the new triangulation \mathcal{T}_{l+1} .

Example 4.1. (*L*-shape domain with manufactured solution) Let $\Omega = (-1, 1) \times (-1, 1) \setminus [0, 1] \times [-1, 0]$. Consider (1.2) with the manufactured solution presented in Example 3.2, with the parameter $\epsilon = 1$ and apply the adaptive refinement algorithm. We account for the non-zero right hand side \mathbf{f} , calculated using this manufactured solution, by modifying the estimator to be $\vartheta_T^2 := h_T^2 \|\mathbf{f} - 2\epsilon^{-2}(|\Psi_h|^2 - 1)\Psi_h\|_{0,T}^2$. Figure 2a displays the initial triangulations. Figures 2b and 2c plot the discrete solutions u_h and v_h respectively, and display the adaptive refinement near the vicinity of the re-entrant corner of the L-shaped domain. Table 4

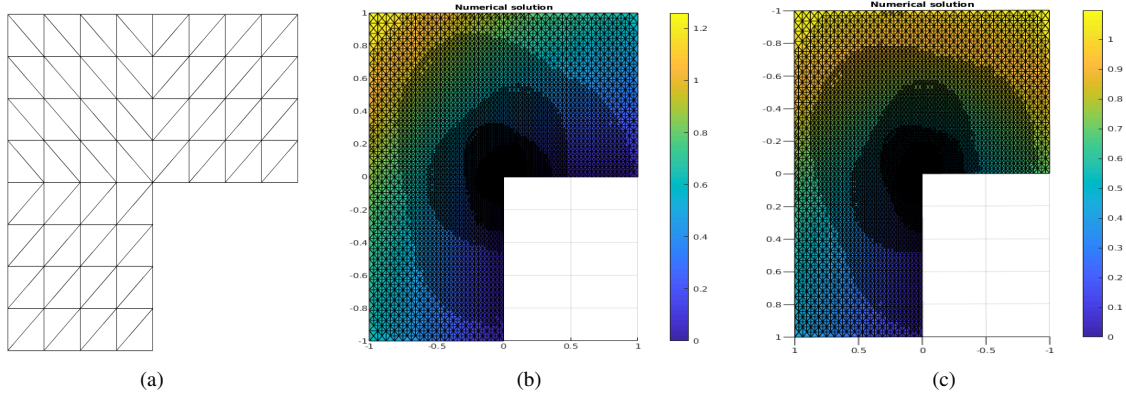


Figure 2: (a) Initial triangulation \mathcal{T}_0 , (b) Adaptive mesh refinement and u_h , (c) Adaptive mesh refinement and v_h .

tabulates the computational error, estimator and convergence rates for uniform and adaptive mesh refinement for the parameter $\epsilon = 1$. It is observed from Table 4 that we have a suboptimal empirical convergence rate (calculated with respect to Ndof) of 0.25 for uniform mesh refinement and an improved optimal empirical convergence rate of 0.5 for adaptive mesh-refinement.

Uniform refinement			Adaptive refinement				
Ndof	Error	Order _e	Ndof	Error	Order _e	ϑ	Order _{ϑ}
42	0.46287	-	42	0.54533	-	0.6494	-
130	0.31420	0.3428	312	0.14827	0.6494	0.57967	0.5450
450	0.21725	0.2971	742	0.08676	0.6185	0.37202	0.5119
1666	0.15082	0.2788	1588	0.05722	0.5471	0.25484	0.4972
6402	0.10495	0.2693	3210	0.03917	0.5385	0.17655	0.5214
25090	0.07319	0.2638	7434	0.02527	0.5217	0.11599	0.5002
99330	0.05115	0.2603	13346	0.01867	0.5166	0.08572	0.5168
395266	0.03582	0.2579	21116	0.01483	0.5015	0.06840	0.4918

Table 4: Numerical errors, estimators and experimental convergence rates for uniform and adaptive mesh refinement for $\epsilon = 1$.

Further, in the adaptive refinement process, the number of mesh points required to achieve convergence is significantly reduced compared to uniform meshes and the convergence is faster than the uniform refinement process. Figure 3 displays the convergence behavior of the error and estimator along with the reliability constant C_{rel} plot, as a function of the total number of degrees of freedoms for $\epsilon = 0.2, 0.8$. Here, C_{rel} is the ratio between computed errors and estimators which remains constant after the first few refinement levels. The tolerance used for Newton's method convergence is 10^{-12} in this example.

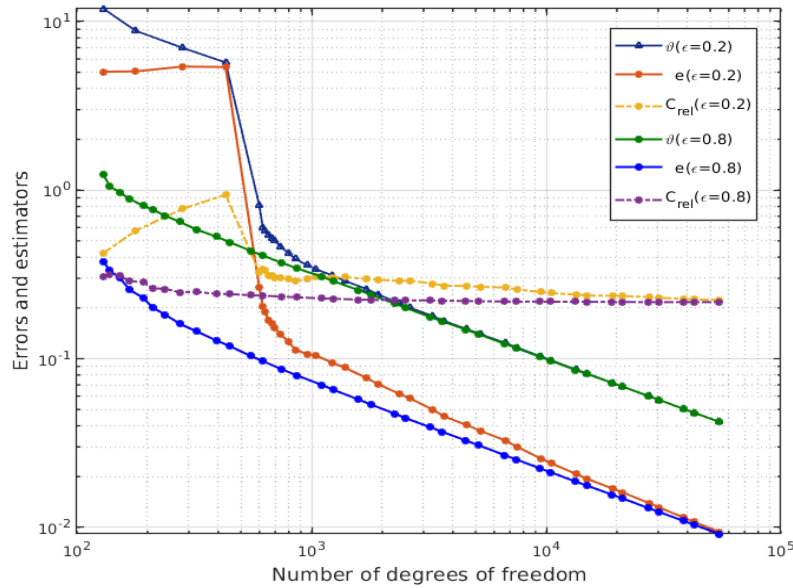


Figure 3: Ndof versus e , ϑ and C_{rel} for Example 4.1.

Example 4.2. (Square domain with benchmark example) Consider (1.2) in a square domain $\Omega = (0, 1) \times (0, 1)$, with boundary data as in Example 3.1 and apply the adaptive refinement algorithm to recover the diagonal and rotated solutions corresponding to the planar bistable liquid crystal device. Figures 4 and 5 display the discrete solutions (diagonal D1 and rotated R1, respectively) along with the adaptive mesh refinement and the director field plots. Here, we observe adaptive mesh refinements near the defect points [37] of the domain (four corner points) and the estimator tends to zero as the number of degrees of freedom (Ndof) increases. Figure 6 is the estimator vs Ndof plot for various values of ϵ for the rotated, R1 solution. The tolerance used for Newton's method convergence is 10^{-6} and it is observed that the number of Newton iterations required for the convergence varies for various values of ϵ as expected from Theorem 3.18.

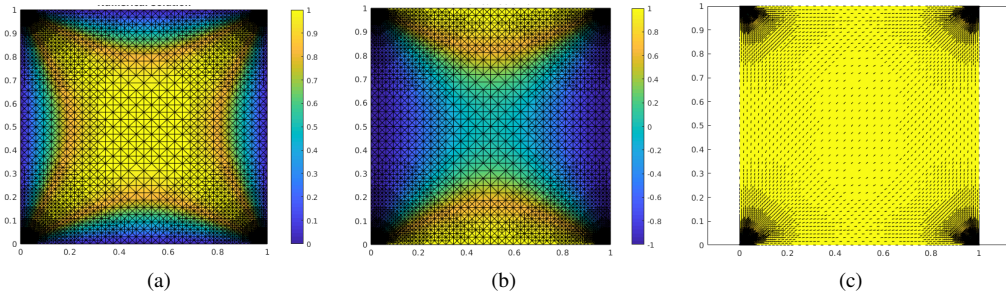


Figure 4: D1 solution: (a) Adaptive mesh refinement and u_h . (b) Adaptive mesh refinement and v_h . (c) Director field plot.

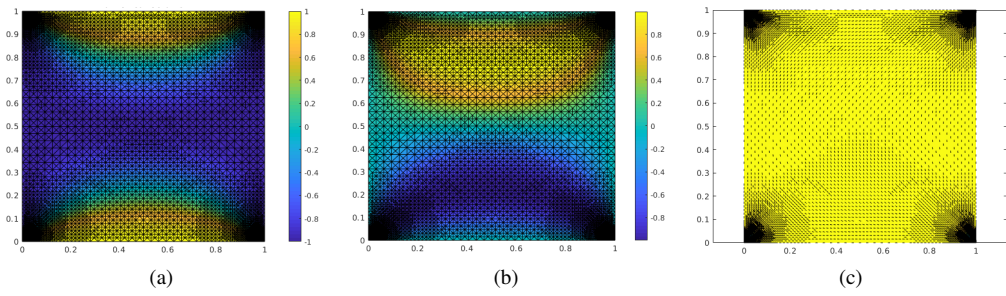


Figure 5: R1 solution: (a) Adaptive mesh refinement and u_h . (b) Adaptive mesh refinement and v_h . (c) Director field plot.

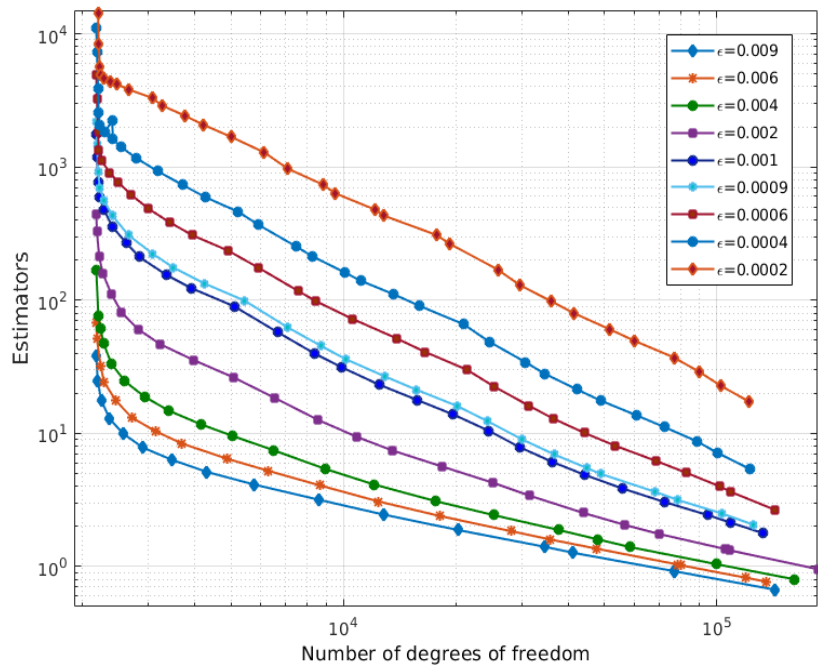


Figure 6: Estimator vs N dof plot for various values of ϵ in square domain.

Since the exact solution is not known for this example, we plot only the estimator as a function of degrees of freedom. The errors, as a function of the N dof, are expected to mirror the trends of the associated estimators

and to be parallel to the estimator plots from theoretical estimates. Observe that the rate of decay of the estimators is slower for smaller values of ϵ .

Remark 4.6. The h - ϵ dependency discussed in [39] has been reflected for adaptive refinement in this article in terms of N dof- ϵ dependency. The authors observed in [39] that errors are sensitive to the choice of discretization parameter as ϵ decreases.

Example 4.3. (*L*-shape domain liquid crystal example) Consider (1.2) in a *L*-shape domain $\Omega = (-1, 1) \times (-1, 1) \setminus [0, 1] \times [-1, 0]$ with the tangential boundary condition prescribed below. Label the edges of Ω as C_1, C_2, C_3, C_4, C_5 and C_6 counterclockwise starting from $(0, 0)$. The director $\mathbf{n} = (\cos \theta, \sin \theta)$ is constrained to be tangent to the boundary edges. Set $\theta = 0$ on C_1, C_3, C_5 and $\theta = -\frac{\pi}{2}$ on C_2, C_4, C_6 , leading to the

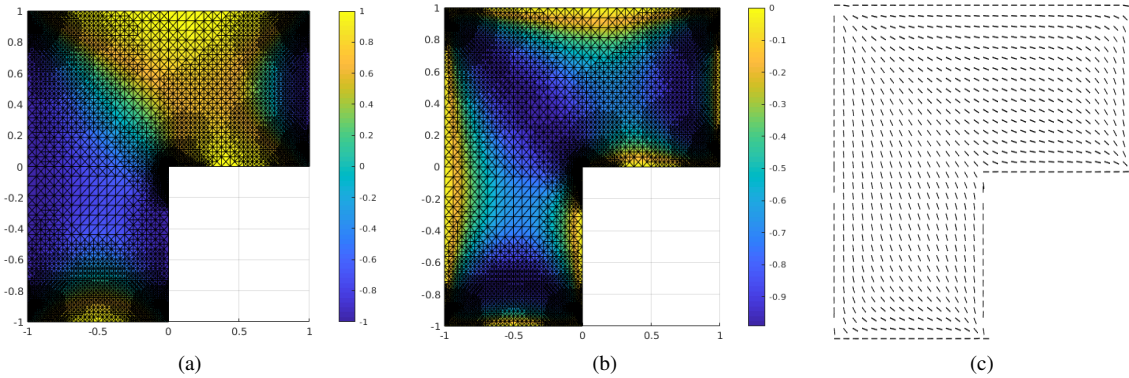


Figure 7: (a) Adaptive mesh refinement and u_h . (b) Adaptive mesh refinement and v_h . (c) Director field plot.

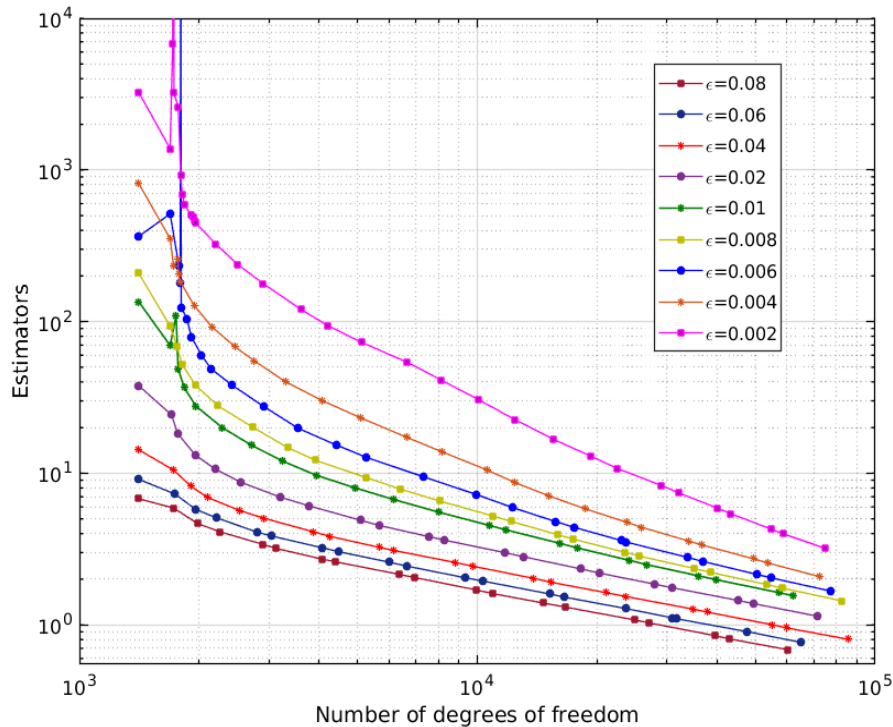


Figure 8: Estimator vs N dof plot for various values of ϵ in *L*-shape domain.

director field in 7c. The boundary function \mathbf{g} is constructed using the trapezoidal shape function $T_d(\cdot)$, with

$d = 3\epsilon$ in (3.47) and is defined by

$$\mathbf{g} = \begin{cases} (T_d(x), 0) & \text{on } C_1, C_3 \text{ and } C_5, \\ (-T_d(y), 0) & \text{on } C_2, C_4 \text{ and } C_6. \end{cases}$$

To compute the initial guess $\Psi_h^0 = s(\cos \theta, \sin \theta)$, we first solve $\Delta \theta = 0$ in Ω with the boundary conditions described above, using Nitsche's method and choose $s = |\mathbf{g}|$ on boundary edges and $s = 1$ in the interior domain. Figure 7 plots the level curves of the converged solution components, u_h, v_h , in the L-shape domain along with adaptive refinements and the corresponding director fields. Figure 8 illustrated the convergence trends of the estimators as a function of the number of degrees of freedom, for different values of ϵ . The tolerance used for Newton's method convergence in this numerical experiment is 10^{-12} . The convergence rate of the estimator is 0.5, for $\epsilon = 0.08$. As expected, the rate of decay of the estimator is slower for smaller values of ϵ .

5 Conclusions

This manuscript focuses on *a priori* and *a posteriori* error analysis for solutions with milder regularity than \mathbf{H}^2 , and such solutions of lesser regularity are relevant, for example, in polygonal domains or domains with re-entrant corners that have boundary conditions of lesser regularity. We use Nitsche's method for our analysis; the *a priori* error analysis relies on medius analysis and these techniques can be extended to other methods too, e.g. discontinuous Galerkin finite element methods. In [39], h - ϵ dependent error estimates for $\mathbf{H}^2(\Omega)$ regular solutions are obtained, and this follows from an ϵ independent bound for the exact solution $\|\Psi\|_2$, as established in [7]. It is not clear if such estimates are feasible for exact solutions with milder regularity, $\mathbf{H}^{1+\alpha}(\Omega)$, $\alpha \in (0, 1]$, since we do not have ϵ -independent bounds for $\|\Psi\|_{1+\alpha}$ at hand. It may be possible to obtain such bounds for certain model problems, which would allow $h - \epsilon$ dependent estimates. There are several future directions for challenging research - convergence of adaptive algorithms, applications of our theoretical estimates to benchmark problems for liquid crystals in complex geometries with complex boundary conditions, use of these estimates in the design of new numerical algorithms to test their stability and robustness and wider applications to problems in materials science or phase-field models. The overarching aim is to propose optimal estimates for the discretization parameter and number of degrees of freedom as a function of the model parameters and solution variables, and use these estimates for powerful new computational algorithms.

Acknowledgements

R.M. gratefully acknowledges support from institute Ph.D. fellowship and N.N. gratefully acknowledges support from the Faculty of Science at the University of Bath and the support by DST SERB MATRICS grant MTR/2017/000 199. A.M acknowledges support from the DST-UKIERI and British Council funded project on "Theoretical and Experimental Studies of Suspensions of Magnetic Nanoparticles, their Applications and Generalizations" and support from IIT Bombay, and a Visiting Professorship from the University of Bath.

References

- [1] J. H. Adler, T. J. Atherton, D. B. Emerson, and S. P. MacLachlan, *An energy-minimization finite-element approach for the Frank-Oseen model of nematic liquid crystals*, SIAM Journal on Numerical Analysis **53** (2015), no. 5, 2226–2254.
- [2] M. Ainsworth and J. T. Oden, *A posteriori error estimation in finite element analysis*, Pure and Applied Mathematics (New York), Wiley-Interscience [John Wiley & Sons], New York, 2000.
- [3] C. Bacuta, J. H. Bramble, and J. Xu, *Regularity estimates for elliptic boundary value problems in Besov spaces*, Mathematics of Computation **72** (2003), no. 244, 1577–1595.
- [4] J. M. Ball and A. Majumdar, *Nematic liquid crystals: From maier-saupe to a continuum theory*, Molecular Crystals and Liquid Crystals **525** (2010), no. 1, 1–11.

- [5] S. Bartels, C. Carstensen, and G. Dolzmann, *Inhomogeneous Dirichlet conditions in a priori and a posteriori finite element error analysis*, *Numerische Mathematik* **99** (2004), no. 1, 1–24.
- [6] R. Becker, P. Hansbo, and R. Stenberg, *A finite element method for domain decomposition with non-matching grids*, *M2AN. Mathematical Modelling and Numerical Analysis* **37** (2003), no. 2, 209–225.
- [7] F. Bethuel, H. Brezis, and F. Hélein, *Asymptotics for the minimization of a Ginzburg-Landau functional*, *Calculus of Variations and Partial Differential Equations* **1** (1993), no. 2, 123–148.
- [8] ———, *Ginzburg-Landau vortices*, *Progress in Nonlinear Differential Equations and their Applications*, vol. 13, Birkhäuser Boston, Inc., Boston, MA, 1994.
- [9] D. Braess and R. Verfürth, *A posteriori error estimators for the Raviart-Thomas element*, *SIAM Journal on Numerical Analysis* **33** (1996), no. 6, 2431–2444.
- [10] S. C. Brenner, *Poincaré-Friedrichs inequalities for piecewise H^1 functions*, *SIAM Journal on Numerical Analysis* **41** (2003), no. 1, 306–324.
- [11] S. C. Brenner and L. R. Scott, *The mathematical theory of finite element methods*, Third ed., *Texts in Applied Mathematics*, vol. 15, Springer, New York, 2008.
- [12] C. Carstensen, S. Bartels, and S. Jansche, *A posteriori error estimates for nonconforming finite element methods*, *Numerische Mathematik* **92** (2002), no. 2, 233–256.
- [13] C. Carstensen, R. Lazarov, and S. Tomov, *Explicit and averaging a posteriori error estimates for adaptive finite volume methods*, *SIAM Journal on Numerical Analysis* **42** (2005), no. 6, 2496–2521.
- [14] C. Carstensen, G. Mallik, and N. Nataraj, *A priori and a posteriori error control of discontinuous Galerkin finite element methods for the von Kármán equations*, *IMA J. Numer. Anal.* **39** (2019), no. 1, 167–200.
- [15] ———, *Nonconforming finite element discretisation for semilinear problems with trilinear nonlinearity*, (2019).
- [16] P. G. Ciarlet, *The finite element method for elliptic problems*, *Classics in Applied Mathematics*, vol. 40, Society for Industrial and Applied Mathematics (SIAM), Philadelphia, PA, 2002.
- [17] T. A. Davis and E. C. Gartland, Jr., *Finite element analysis of the Landau-de Gennes minimization problem for liquid crystals*, *SIAM Journal on Numerical Analysis* **35** (1998), no. 1, 336–362.
- [18] P.G. de Gennes and J. Prost, *The physics of liquid crystals*, *International Series of Monographs*, Clarendon Press, 1993.
- [19] G. Di Fratta, J. M. Robbins, V. Slastikov, and A. Zarnescu, *Half-integer point defects in the Q -tensor theory of nematic liquid crystals*, *Journal of Nonlinear Science* **26** (2016), no. 1, 121–140.
- [20] D. A. Di Pietro and A. Ern, *Mathematical aspects of discontinuous Galerkin methods*, *Mathématiques & Applications (Berlin) [Mathematics & Applications]*, vol. 69, Springer, Heidelberg, 2012.
- [21] J. L. Ericksen, *Liquid crystals with variable degree of orientation*, *Archive for Rational Mechanics and Analysis* **113** (1990), no. 2, 97–120.
- [22] A. Ern and J-L. Guermond, *Theory and practice of finite elements*, *Applied Mathematical Sciences*, vol. 159, Springer-Verlag, New York, 2004.
- [23] L. C. Evans, *Partial differential equations*, second ed., *Graduate Studies in Mathematics*, vol. 19, American Mathematical Society, Providence, RI, 2010.
- [24] D. Golovaty, J. A. Montero, and P. Sternberg, *Dimension reduction for the Landau-de Gennes model in planar nematic thin films*, *Journal of Nonlinear Science* **25** (2015), no. 6, 1431–1451.
- [25] P. Grisvard, *Singularities in boundary value problems*, *Recherches en Mathématiques Appliquées [Research in Applied Mathematics]*, vol. 22, Masson, Paris; Springer-Verlag, Berlin, 1992.

- [26] T. Gudi, *A new error analysis for discontinuous finite element methods for linear elliptic problems*, Mathematics of Computation **79** (2010), no. 272, 2169–2189.
- [27] D. Henao, A. Majumdar, and A. Pisante, *Uniaxial versus biaxial character of nematic equilibria in three dimensions*, Calculus of Variations and Partial Differential Equations **56** (2017), no. 2, Art. 55, 22.
- [28] M. Juntunen and R. Stenberg, *Nitsche’s method for general boundary conditions*, Mathematics of Computation **78** (2009), no. 267, 1353–1374.
- [29] O. A. Karakashian and F. Pascal, *A posteriori error estimates for a discontinuous Galerkin approximation of second-order elliptic problems*, SIAM Journal on Numerical Analysis **41** (2003), no. 6, 2374–2399.
- [30] H. B. Keller, *Approximation methods for nonlinear problems with application to two-point boundary value problems*, Mathematics of Computation **29** (1975), 464–474.
- [31] S. Kesavan, *Topics in functional analysis and applications*, John Wiley & Sons, Inc., New York, 1989.
- [32] K. Y. Kim, *A posteriori error analysis for locally conservative mixed methods*, Mathematics of Computation **76** (2007), no. 257, 43–66.
- [33] ———, *A posteriori error estimators for locally conservative methods of nonlinear elliptic problems*, Applied Numerical Mathematics. An IMACS Journal **57** (2007), no. 9, 1065–1080.
- [34] A. Lasis and E. Süli, *Poincaré-type inequalities for broken obolev spaces*, Technical Report 03/10, Oxford University Computing Laboratory, Oxford, England (2003).
- [35] F. Lin and C. Liu, *Static and dynamic theories of liquid crystals*, Journal of Partial Differential Equations **14** (2001), no. 4, 289–330.
- [36] J.-L. Lions and E. Magenes, *Non-homogeneous boundary value problems and applications. Vol. I*, Springer-Verlag, New York-Heidelberg, 1972, Translated from the French by P. Kenneth, Die Grundlehren der mathematischen Wissenschaften, Band 181.
- [37] C. Luo, A. Majumdar, and R. Erban, *Multistability in planar liquid crystal wells*, Physics Review E **85** (2012), 061702.
- [38] N. Lüthen, M. Juntunen, and R. Stenberg, *An improved a priori error analysis of Nitsche’s method for Robin boundary conditions*, Numer. Math. **138** (2018), no. 4, 1011–1026.
- [39] R. R. Maity, A. Majumdar, and N. Nataraj, *Discontinuous Galerkin finite element methods for the Landau-de Gennes minimization problem of liquid crystals*, (2020).
- [40] A. Majumdar and A. Zarnescu, *Landau-de Gennes theory of nematic liquid crystals: the Oseen-Frank limit and beyond*, Archive for Rational Mechanics and Analysis **196** (2010), no. 1, 227–280.
- [41] J. Nitsche, *Über ein variationsprinzip zur lösung von dirichlet-problemen bei verwendung von teilträumen, die keinen randbedingungen unterworfen sind*, Abhandlungen aus dem Mathematischen Seminar der Universität Hamburg **36** (1971), no. 1, 9–15.
- [42] F. Pacard and T. Rivière, *Linear and nonlinear aspects of vortices: The Ginzburg-Landau model*, Progress in Nonlinear Differential Equations and Their Applications, Birkhäuser, 2000.
- [43] S. Prudhomme, F. Pascal, J. T. Oden, and A. Romkes, *A priori error estimate for the Baumann-Oden version of the discontinuous Galerkin method*, Comptes Rendus de l’Académie des Sciences. Série I. Mathématique **332** (2001), no. 9, 851–856.
- [44] L. R. Scott and S. Zhang, *Finite element interpolation of nonsmooth functions satisfying boundary conditions*, Mathematics of Computation **54** (1990), no. 190, 483–493.
- [45] C. Tsakonas, A. J. Davidson, C. V. Brown, and N. J. Mottram, *Multistable alignment states in nematic liquid crystal filled wells*, Applied Physics Letters **90** (2007), Article 111913.

- [46] R. Verfürth, *A posteriori error estimation techniques for finite element methods*, Numerical Mathematics and Scientific Computation, Oxford University Press, Oxford, 2013.
- [47] Y. Wang, G. Canevari, and A. Majumdar, *Order reconstruction for nematics on squares with isotropic inclusions: a Landau–de Gennes study*, SIAM J. Appl. Math. **79** (2019), no. 4, 1314–1340.

A Appendix

A.1 Boundedness properties

Proof of Lemma 3.8. (i) The definition of $B_h(\cdot, \cdot, \cdot, \cdot)$, a regrouping of terms and (3.7) lead to

$$\begin{aligned} B_h(\eta_h, \eta_h, \eta_h, \Phi_h) - B_h(\eta, \eta, \eta, \Phi_h) &= \sum_{T \in \mathcal{T}} (B_T(\eta_h - \eta, \eta_h - \eta, \eta_h, \Phi_h) + 2B_T(\eta_h - \eta, \eta_h - \eta, \eta, \Phi_h) \\ &+ 3B_T(\eta, \eta, \eta_h - \eta, \Phi_h)) \lesssim \epsilon^{-2} (\|\eta_h - \eta\|_h^2 \|\eta_h\|_h + \|\eta_h - \eta\|_h^2 \|\eta\|_1 + \|\eta_h - \eta\|_h \|\eta\|_1^2) \|\Phi_h\|_h. \end{aligned}$$

(ii) For $\eta \in \mathbf{H}^{1+\alpha}(\Omega)$ with $\alpha > 0$ and $\eta_h = \mathbf{I}_h \eta$, a use of (3.8) and Remark 3.5 lead to

$$\begin{aligned} B_h(\mathbf{I}_h \eta, \mathbf{I}_h \eta, \mathbf{I}_h \eta, \Phi_h) - B_h(\eta, \eta, \eta, \Phi_h) &\lesssim \epsilon^{-2} (\|\mathbf{I}_h \eta - \eta\|_h^2 \|\mathbf{I}_h \eta\|_h + \|\mathbf{I}_h \eta - \eta\|_h^2 \|\eta\|_{1+\alpha}) \|\Phi_h\|_h \\ &+ \|\mathbf{I}_h \eta - \eta\|_0 \|\eta\|_{1+\alpha}^2 \|\Phi_h\|_0 \lesssim \epsilon^{-2} \|\eta\|_{1+\alpha}^3 (h^{2\alpha} \|\Phi_h\|_h + h^{1+\alpha} \|\Phi_h\|_0). \end{aligned}$$

(iii) The definition of $B_h(\cdot, \cdot, \cdot, \cdot)$, a regrouping of terms, (3.6) and Remark 3.5 lead to

$$\begin{aligned} B_h(\eta, \eta, \Theta_h, \Phi_h) - B_h(\mathbf{I}_h \eta, \mathbf{I}_h \eta, \Theta_h, \Phi_h) &= \frac{2}{3\epsilon^2} \sum_{T \in \mathcal{T}_h} \int_T ((\eta - \mathbf{I}_h \eta) \cdot (\eta + \mathbf{I}_h \eta)) (\Theta_h \cdot \Phi_h) \\ &+ 2(\eta - \mathbf{I}_h \eta) \cdot \Theta_h (\eta \cdot \Phi_h) + 2(\mathbf{I}_h \eta \cdot \Theta_h) (\eta - \mathbf{I}_h \eta) \cdot \Phi_h \, dx \\ &\lesssim \epsilon^{-2} \|\eta - \mathbf{I}_h \eta\|_h \|\eta\|_{1+\alpha} \|\Theta_h\|_h \|\Phi_h\|_h \lesssim \epsilon^{-2} h^\alpha \|\eta\|_{1+\alpha}^2 \|\Theta_h\|_h \|\Phi_h\|_h. \end{aligned}$$

This concludes the proof. \square

A.2 Regularity results

Theorem A.1. [3, 25] *Let Ω be a non-convex polygonal domain in \mathbb{R}^2 , with boundary $\partial\Omega$, and the largest re-entrant corner of measure ω . For $f \in H^{-1+\alpha}(\Omega)$, there exists a $u \in H^{1+\alpha}(\Omega)$ such that $-\Delta u = f$ in Ω and $u = 0$ on $\partial\Omega$ and for $0 < \alpha < s_0 = \frac{\pi}{\omega}$, it holds that $\|u\|_{1+\alpha} \leq C(\alpha) \|f\|_{-1+\alpha}$. Here the norms involved are the standard Sobolev fractional norms.*

Proof of Lemma 3.10. The first part of the proof follows analogous to the proof in Theorem 4.7 of [39]. For $\Theta_h \in \mathbf{X}_h$, Lemma 3.7 implies $B_h(\Psi, \Psi, \Theta_h, \cdot)$, $B(\Psi, \Psi, \Pi_h \Theta_h, \cdot)$, $C_h(\Theta_h, \cdot)$, $C(\Pi_h \Theta_h, \cdot) \in \mathbf{L}^2(\Omega)$. Therefore, a use of Theorem A.1 and $\|\Theta_h\|_h = 1$ yields that there exist $\xi, \eta \in \mathbf{H}^{1+\alpha}(\Omega) \cap \mathbf{V}$ that solves (3.10), (3.11) and satisfies

$$\|\xi\|_{1+\alpha} \lesssim \|B_h(\Psi, \Psi, \Theta_h, \cdot) + C_h(\Theta_h, \cdot)\|_{-1+\alpha} \lesssim \|B_h(\Psi, \Psi, \Theta_h, \cdot) + C_h(\Theta_h, \cdot)\|_0 \lesssim \epsilon^{-2} (1 + \|\Psi\|_{1+\alpha}^2).$$

To prove the second inequality in (3.12), we subtract (3.10) from (3.11) with a choice of $\Phi = \eta - \xi$ and use Poincaré inequality in Lemma 3.1.

$$\|\nabla(\eta - \xi)\|_0 \lesssim \epsilon^{-2} (1 + \|\Psi\|_{1+\alpha}^2) \|\Theta_h - \Pi_h \Theta_h\|_0. \quad (\text{A.1})$$

A use of (3.1) in (A.1) concludes the proof. \square

Theorem A.2. *Let Ω be a non-convex polygonal domain in \mathbb{R}^2 . For $f \in H^{-1+\alpha}(\Omega)$ and $g \in H^{\frac{1}{2}+\alpha}(\partial\Omega)$ with $0 < \alpha < 1$, there exists a $u \in H^{1+\alpha}(\Omega)$ such that*

$$-\Delta u = f \text{ in } \Omega \text{ and } u = g \text{ on } \partial\Omega. \quad (\text{A.2})$$

Proof. For $g \in H^{\frac{1}{2}+\alpha}(\partial\Omega)$, a use of Trace theorem [36, Page 41] yields that there exists $u_g \in H^{1+\alpha}(\Omega)$ such that $u_g = g$ on $\partial\Omega$. Let $\tilde{u} = u - u_g$. The weak formulation of (A.2) is given by

$$\int_{\Omega} \nabla \tilde{u} \cdot \nabla v \, dx = \int_{\Omega} f v \, dx - \int_{\Omega} \nabla u_g \cdot \nabla v \, dx \text{ for all } v \in H_0^1(\Omega).$$

Since $u_g \in H^{1+\alpha}(\Omega)$, $\Delta u_g \in H^{-1+\alpha}(\Omega)$ by real interpolation of Sobolev spaces [11]. A use of Theorem A.1 leads to the existence of the solution $\tilde{u} \in H^{1+\alpha}(\Omega)$. This together with $u_g \in H^{1+\alpha}(\Omega)$ yields the existence of the solution u of (A.2) with $u \in H^{1+\alpha}(\Omega)$. \square

Lemma A.3. *Let Ω be a non-convex polygonal domain of \mathbb{R}^2 . Then for $\mathbf{g} \in \mathbf{H}^{\frac{1}{2}+\alpha}(\partial\Omega)$ with $0 < \alpha < 1$, any solution of (1.2) belongs to $\mathbf{H}^{1+\alpha}(\Omega)$.*

Proof. Rewrite the system (1.2) as: $-\Delta \Psi = F_1(\Psi)$ in Ω and $\Psi = \mathbf{g}$ on $\partial\Omega$, where $F_1(\Psi) = 2\epsilon^{-2}(1 - |\Psi|^2)\Psi$. Expand the expression for $F_1(\Psi)$, where $\Psi = (u, v) \in \mathbf{H}^1(\Omega)$, use the Sobolev embedding result $H^1(\Omega) \hookrightarrow L^p(\Omega)$ for all $p \geq 1$, and the Hölder's inequality to prove that $F_1(\Psi) \in \mathbf{L}^2(\Omega) \subset \mathbf{H}^{-1+\alpha}(\Omega)$ with $0 < \alpha < 1$. Now a use of Theorem A.2 and a bootstrapping argument [23] imply that the solution Ψ of (1.2) belongs to $\mathbf{H}^{1+\alpha}(\Omega)$. \square

A.3 Local efficiency

Since the estimator is used to be the basis of adaptive refinement algorithm, it is expected that the estimator is efficient in the sense of Theorem 2.3. The local cut off functions play an important role to establish the local efficiency results. Consider the interior bubble function [2, 46] $b_T = 27\lambda_1\lambda_2\lambda_3$ supported on a reference triangle \hat{T} with the barycentric coordinate functions $\hat{\lambda}_1, \hat{\lambda}_2, \hat{\lambda}_3$. For $T \in \mathcal{T}$, let $\mathcal{F}_T : \hat{T} \rightarrow T$ be a continuous, affine and invertible transformation. Define the bubble function on the element T by $b_T = \hat{b}_T \circ \mathcal{F}_T^{-1}$. Three edge bubble functions on the reference triangle \hat{T} are given by $\hat{b}_1 = 4\hat{\lambda}_2\hat{\lambda}_3$, $\hat{b}_2 = 4\hat{\lambda}_1\hat{\lambda}_3$ and $\hat{b}_3 = 4\hat{\lambda}_1\hat{\lambda}_2$. On the edge E of any triangle $T \in \mathcal{T}$, define the edge bubble function to be $b_E := \hat{b}_E \circ \mathcal{F}_T^{-1}$, where \hat{b}_E is the corresponding edge bubble function on \hat{T} . Here, b_E is supported on the pair of triangles sharing the edge E .

Lemma A.4. [2, 46] *Let $\hat{P} \subset H^1(\hat{T})$ be a finite dimensional subspace on the reference triangle \hat{T} and consider $P = \{\hat{v} \circ \mathcal{F}_T^{-1} : \hat{v} \in \hat{P}\}$ to be the finite dimensional space of functions defined on T . Then the following inverse estimates hold for all $v \in P$,*

$$\|v\|_{L^2(T)}^2 \lesssim \int_T b_T v^2 \, dx \lesssim \|v\|_{L^2(T)}^2, \quad \|v\|_{L^2(T)} \lesssim \|b_T v\|_{L^2(T)} + h_T \|\nabla(b_T v)\|_{L^2(T)} \lesssim \|v\|_{L^2(T)}. \quad (\text{A.3})$$

Let $E \subset \partial T$ be an edge and b_E be the corresponding edge bubble function supported on the patch of triangles ω_E sharing the edge E . Let $P(E)$ be the finite dimensional space of functions defined on E obtained by mapping $\hat{P}(\hat{E}) \subset H^1(\hat{E})$. Then for all $v \in P(E)$

$$\|v\|_{L^2(E)}^2 \lesssim \int_E b_E v^2 \, dx \lesssim \|v\|_{L^2(E)}^2, \quad h_E^{-\frac{1}{2}} \|b_E v\|_{L^2(\omega_E)} + h_E^{\frac{1}{2}} \|\nabla(b_E v)\|_{L^2(\omega_E)} \lesssim \|v\|_{L^2(E)}, \quad (\text{A.4})$$

where the hidden constants in " \lesssim " are independent of h_T and h_E .

Proof of Lemma 3.9. (i) Let $T \in \mathcal{T}$ be arbitrary and b_T be the interior bubble function supported on the triangle T . Define

$$\rho_T = \begin{cases} (-\Delta \Phi_h + 2\epsilon^{-2}(|\Phi_h|^2 - 1)\Phi_h) b_T & \text{in } T, \\ 0 & \text{in } \Omega \setminus T. \end{cases}$$

The results in (A.3), (2.1) with $\Phi := \rho_T$ and an integration by parts of the first term (which is a zero term) on the right-hand side below lead to

$$\begin{aligned} \|\eta_T\|_{0,T}^2 &\lesssim \int_T (-\Delta \Phi_h + 2\epsilon^{-2}(|\Phi_h|^2 - 1)\Phi_h) \cdot \rho_T \, dx \\ &= A_T(\Phi_h, \rho_T) + B_T(\Phi_h, \Phi_h, \Phi_h, \rho_T) + C_T(\Phi_h, \rho_T) - A_T(\Psi, \rho_T) - B_T(\Psi, \Psi, \Psi, \rho_T) - C_T(\Psi, \rho_T) \\ &= A_T(\Phi_h - \Psi, \rho_T) + (B_T(\Phi_h, \Phi_h, \Phi_h, \rho_T) - B_T(\Psi, \Psi, \Psi, \rho_T)) + C_T(\Phi_h - \Psi, \rho_T). \end{aligned} \quad (\text{A.5})$$

Together with Hölder's inequality, Lemma 3.8(i) and (A.3), the terms on the right hand side of (A.5) are estimated as

$$A_T(\Phi_h - \Psi, \rho_T) \lesssim \|\nabla(\Phi_h - \Psi)\|_{0,T} \|\nabla \rho_T\|_{0,T} \lesssim \|\Psi - \Phi_h\|_{1,T} h_T^{-1} \|\eta_T\|_{0,T}. \quad (\text{A.6})$$

$$C_T(\Phi_h - \Psi, \rho_T) \lesssim \epsilon^{-2} \|\Phi_h - \Psi\|_{0,T} \|\rho_T\|_{0,T} \lesssim \epsilon^{-2} \|\Psi - \Phi_h\|_{0,T} \|\eta_T\|_{0,T}, \quad (\text{A.7})$$

$$\begin{aligned} B_T(\Phi_h, \Phi_h, \Phi_h, \rho_T) - B_T(\Psi, \Psi, \Psi, \rho_T) &\lesssim \epsilon^{-2} \|\Psi - \Phi_h\|_{1,T} (\|\Psi - \Phi_h\|_{1,T} (\|\Phi_h\|_{1,T} + \|\Psi\|_{1,T})) \\ &\quad + \|\Psi\|_{1,T}^2 h_T^{-1} \|\eta_T\|_{0,T}. \end{aligned}$$

A combination the above three displayed estimates in (A.5) and Lemma A.4 establishes

$$h_T \|\eta_T\|_{0,T} \lesssim \|\Psi - \Phi_h\|_{h,T} (1 + \epsilon^{-2} (1 + \|\Psi\|_{1,T}^2 + \|\Psi - \Phi_h\|_{h,T} (\|\Phi_h\|_{1,T} + \|\Psi\|_{1,T}))). \quad (\text{A.8})$$

To find the estimate corresponding to η_E , consider the edge bubble function b_E supported on the patch of triangles ω_E sharing the edge E . Define

$$\rho_E = \begin{cases} [\nabla \Phi_h \nu] b_E & \text{in } \omega_E, \\ 0 & \text{in } \Omega \setminus \omega_E. \end{cases}$$

A use of (A.4), $[\rho_E] = 0$ for $E \in \mathcal{E}_h^i$ and an integration by parts lead to

$$\begin{aligned} \|\eta_E\|_{0,E}^2 &\lesssim \int_E [\nabla \Phi_h \nu] \cdot \rho_E \, ds = \int_E [\nabla \Phi_h \nu] \cdot \{\rho_E\} \, ds + \int_E \{\nabla \Phi_h \nu\} \cdot [\rho_E] \, ds \\ &= \sum_{T \in \omega_E} \int_T (\Delta \Phi_h \cdot \rho_E + \nabla \Phi_h \cdot \nabla \rho_E) \, dx. \end{aligned} \quad (\text{A.9})$$

Now we add and subtract $\sum_{T \in \omega_E} \int_T 2\epsilon^{-2} (|\Phi_h|^2 - 1) \Phi_h \cdot \rho_E \, dx$ in (A.9) to rewrite the expression with the help of $\eta_T = \Delta \Phi_h - 2\epsilon^{-2} (|\Phi_h|^2 - 1) \Phi_h$ (with a $-\Delta \Phi_h = 0$ added). The expression (2.1) with $\Phi = \rho_E$, a re-grouping of terms and Hölder's inequality lead to

$$\begin{aligned} \|\eta_E\|_{0,E}^2 &\lesssim \left(\sum_{T \in \omega_E} \|\eta_T\|_{0,T}^2 \right)^{\frac{1}{2}} \left(\sum_{T \in \omega_E} \|\rho_E\|_{0,T}^2 \right)^{\frac{1}{2}} + \sum_{T \in \omega_E} (A_T(\Phi_h - \Psi, \rho_E) + C_T(\Phi_h - \Psi, \rho_E)) \\ &\quad + (B_T(\Phi_h, \Phi_h, \Phi_h, \rho_E) - B_T(\Psi, \Psi, \Psi, \rho_E)). \end{aligned} \quad (\text{A.10})$$

A combination of Hölder's inequality, Lemma 3.8(i) and (A.4) yields

$$\sum_{T \in \omega_E} A_T(\Phi_h - \Psi, \rho_E) \lesssim \sum_{T \in \omega_E} \|\nabla(\Psi - \Phi_h)\|_{0,T} \|\nabla \rho_E\|_{0,T} \lesssim h_E^{-\frac{1}{2}} \|\eta_E\|_{0,E} \|\nabla(\Psi - \Phi_h)\|_{0,\omega_E}, \quad (\text{A.11})$$

$$\sum_{T \in \omega_E} C_T(\Phi_h - \Psi, \rho_E) \lesssim \epsilon^{-2} \sum_{T \in \omega_E} \|\Psi - \Phi_h\|_{0,T} \|\rho_E\|_{0,T} \lesssim \epsilon^{-2} h_E^{\frac{1}{2}} \|\eta_E\|_{0,E} \|\Psi - \Phi_h\|_{0,\omega_E}, \quad (\text{A.12})$$

$$\begin{aligned} \sum_{T \in \omega_E} (B_T(\Phi_h, \Phi_h, \Phi_h, \rho_E) - B_T(\Psi, \Psi, \Psi, \rho_E)) &\lesssim \epsilon^{-2} h_E^{-\frac{1}{2}} \|\eta_E\|_{0,E} \sum_{T \in \omega_E} \|\Psi - \Phi_h\|_{1,T} (\|\Psi - \Phi_h\|_{1,T} (\|\Phi_h\|_{1,T} \\ &\quad + \|\Psi\|_{1,T}) + \|\Psi\|_{1,T}^2). \end{aligned}$$

The estimate of $\|\eta_T\|_{0,T}$ in (A.8) and (A.4) together with the above three displayed estimates in (A.10) lead to

$$h_E^{\frac{1}{2}} \|\eta_E\|_{0,E} \lesssim \sum_{T \in \omega_E} \|\Psi - \Phi_h\|_{h,T} (1 + \epsilon^{-2} (1 + \|\Psi\|_{1,T}^2 + \|\Psi - \Phi_h\|_{h,T} (\|\Phi_h\|_{1,T} + \|\Psi\|_{1,T}))). \quad (\text{A.13})$$

A combination of (A.8) and A.13 leads to (3.9).

(ii) For $\Phi_h = \mathbf{I}_h \Psi$, a use of Lemma 3.8(ii) and (A.3) yields

$$\begin{aligned} B_T(\mathbf{I}_h \Psi, \mathbf{I}_h \Psi, \mathbf{I}_h \Psi, \rho_T) - B_T(\Psi, \Psi, \Psi, \rho_T) &\lesssim \epsilon^{-2} \|\Psi\|_{1+\alpha,T}^3 (h_T^{2\alpha} \|\nabla \rho_T\|_{0,T} + h_T^{1+\alpha} \|\rho_T\|_{0,T}) \\ &\lesssim \epsilon^{-2} \|\Psi\|_{1+\alpha,T}^3 (h_T^{2\alpha} + h_T^{2+\alpha}) h_T^{-1} \|\eta_T\|_{0,T}. \end{aligned} \quad (\text{A.14})$$

A combination of (A.6), (A.7), (A.14) and Lemma 3.4 leads to

$$\begin{aligned} h_T \|\boldsymbol{\eta}_T\|_{0,T} &\lesssim \|\nabla(\mathbf{I}_h \Psi - \Psi)\|_{0,T} + \epsilon^{-2} \|\mathbf{I}_h \Psi - \Psi\|_{0,T} + \epsilon^{-2} h_T^{2\alpha} \|\Psi\|_{1+\alpha}^3 \\ &\lesssim h_T^\alpha (1 + \epsilon^{-2} h_T^\alpha (1 + \|\Psi\|_{1+\alpha}^2)) \|\Psi\|_{1+\alpha}. \end{aligned} \quad (\text{A.15})$$

Lemma 3.8(ii) and (A.4) yield

$$\begin{aligned} \sum_{T \in \omega_E} (B_T(\mathbf{I}_h \Psi, \mathbf{I}_h \Psi, \mathbf{I}_h \Psi, \boldsymbol{\rho}_E) - B_T(\Psi, \Psi, \Psi, \boldsymbol{\rho}_E)) &\lesssim \epsilon^{-2} \sum_{T \in \omega_E} \|\Psi\|_{1+\alpha,T}^3 (h_T^{2\alpha} \|\nabla \boldsymbol{\rho}_E\|_{0,T} + h_T^{1+\alpha} \|\boldsymbol{\rho}_E\|_{0,T}) \\ &\lesssim \epsilon^{-2} h_E^{-\frac{1}{2}} \|\boldsymbol{\eta}_E\|_{0,E} \sum_{T \in \omega_E} \|\Psi\|_{1+\alpha,T}^3 (h_T^{2\alpha} + h_E h_T^{2+\alpha}). \end{aligned} \quad (\text{A.16})$$

A combination of (A.11), (A.12), (A.12) and Lemma 3.4 leads to

$$h_E^{\frac{1}{2}} \|\boldsymbol{\eta}_E\|_{0,E} \lesssim \sum_{T \in \omega_E} h_T^\alpha (1 + \epsilon^{-2} h_T^\alpha (1 + \|\Psi\|_{1+\alpha}^2)) \|\Psi\|_{1+\alpha}. \quad (\text{A.17})$$

A combination of the estimates in (A.15) and (A.17) concludes the proof of (ii) in Lemma 3.9. \square

Proof of Lemma 3.11. The proof follows similar technique used in Lemmas 3.9 and 3.12 and is presented in brief for the sake of continuity and clarity. Let $T \in \mathcal{T}$ be arbitrary and b_T be the interior bubble function supported on the triangle T . Define

$$\boldsymbol{\rho}_T := \begin{cases} (\Delta(\mathbf{I}_h \boldsymbol{\xi}) + 2\epsilon^{-2}(|\mathbf{I}_h \Psi|^2 \Theta_h + 2(\mathbf{I}_h \Psi \cdot \Theta_h) \mathbf{I}_h \Psi - \Theta_h)) b_T & \text{in } T, \\ 0 & \text{in } \Omega \setminus T. \end{cases}$$

A use of (A.3), (3.10) with $\Phi := \boldsymbol{\rho}_T$, an integration by parts of the first term on the right-hand side below (where $\Delta(\mathbf{I}_h \boldsymbol{\xi}) = 0$ is added) and cancellation of terms lead to

$$\begin{aligned} \|\boldsymbol{\eta}_T\|_{0,T}^2 &\lesssim \int_T (\Delta(\mathbf{I}_h \boldsymbol{\xi}) + 2\epsilon^{-2}(|\mathbf{I}_h \Psi|^2 \Theta_h + 2(\mathbf{I}_h \Psi \cdot \Theta_h) \mathbf{I}_h \Psi - \Theta_h)) \cdot \boldsymbol{\rho}_T \, dx \\ &= A_T(\boldsymbol{\xi} - \mathbf{I}_h \boldsymbol{\xi}, \boldsymbol{\rho}_T) + 3(B_T(\mathbf{I}_h \Psi, \mathbf{I}_h \Psi, \Theta_h, \boldsymbol{\rho}_T) - B_T(\Psi, \Psi, \Theta_h, \boldsymbol{\rho}_T)). \end{aligned}$$

Together with Hölder's inequality, Lemmas 3.4, 3.8(iii) and (3.12) this yields

$$\|\boldsymbol{\eta}_T\|_{0,T}^2 \lesssim h_T^\alpha (\|\boldsymbol{\xi}\|_{1+\alpha,T} + \epsilon^{-2} \|\Psi\|_{1+\alpha,T}^2) h_T^{-1} \|\boldsymbol{\rho}_T\|_{0,T} \lesssim \epsilon^{-2} h_T^\alpha h_T^{-1} (1 + \|\Psi\|_{1+\alpha,T}^2) \|\boldsymbol{\rho}_T\|_{0,T}, \quad (\text{A.18})$$

where (A.3) and $\|\Theta_h\|_h = 1$ are utilized in the first step. Define

$$\boldsymbol{\rho}_E = \begin{cases} [\nabla(\mathbf{I}_h \boldsymbol{\xi})] \nu b_E & \text{in } \omega_E, \\ 0 & \text{in } \Omega \setminus \omega_E. \end{cases}$$

A use of (A.4), $[\boldsymbol{\rho}_E]_E = 0$ for $E \in \mathcal{E}_h^i$ and integration by parts followed by an addition and subtraction of $\sum_{T \in \omega_E} \int_T 2\epsilon^{-2}(|\mathbf{I}_h \Psi|^2 \Theta_h + 2(\mathbf{I}_h \Psi \cdot \Theta_h) \mathbf{I}_h \Psi - \Theta_h) \cdot \boldsymbol{\rho}_E \, dx$ leads to

$$\begin{aligned} \|\boldsymbol{\eta}_E\|_{0,E}^2 &\leq \int_E [\nabla(\mathbf{I}_h \boldsymbol{\xi})] \nu \cdot \boldsymbol{\rho}_E \, ds \lesssim \sum_{T \in \omega_E} \int_T (\Delta(\mathbf{I}_h \boldsymbol{\xi}) + 2\epsilon^{-2}(|\mathbf{I}_h \Psi|^2 \Theta_h + 2(\mathbf{I}_h \Psi \cdot \Theta_h) \mathbf{I}_h \Psi - \Theta_h)) \cdot \boldsymbol{\rho}_E \, dx \\ &\quad + A_T(\mathbf{I}_h \boldsymbol{\xi} - \boldsymbol{\xi}_\epsilon, \boldsymbol{\rho}_E) + 3(B_T(\Psi, \Psi, \Theta_h, \boldsymbol{\rho}_E) - B_T(\mathbf{I}_h \Psi, \mathbf{I}_h \Psi, \Theta_h, \boldsymbol{\rho}_E)). \end{aligned} \quad (\text{A.19})$$

The second term in the right hand side of (A.19) is estimated using Hölder's inequality, Lemma 3.4 and (3.12). The third term is estimated using Lemma 3.8(iii) and $\|\Theta_h\|_h = 1$. Then (A.4) plus the estimate of $\|\boldsymbol{\eta}_T\|_{0,T}$ in (A.18) concludes the proof of the second inequality in Lemma 3.11. \square

Proof of Lemma 3.12. Let $T \in \mathcal{T}$ be arbitrary and b_T be the interior bubble function supported on the triangle T and $G \in \mathbf{X}_h$. Define

$$\boldsymbol{\rho}_T := \begin{cases} (G_h + \Delta(\mathbf{I}_h \boldsymbol{\chi}) - 2\epsilon^{-2}(|\mathbf{I}_h \Psi|^2 \mathbf{I}_h \boldsymbol{\chi} + 2(\mathbf{I}_h \Psi \cdot \mathbf{I}_h \boldsymbol{\chi}) \mathbf{I}_h \Psi - \mathbf{I}_h \boldsymbol{\chi})) b_T & \text{in } T, \\ 0 & \text{in } \Omega \setminus T. \end{cases}$$

A use of (A.3), (3.13) with $\Phi := \rho_T$ and integration by parts of the second term on the right-hand side of the expression below (where $\Delta(\mathbf{I}_h \chi) = 0$) leads to

$$\begin{aligned} \|\boldsymbol{\eta}\|_{0,T}^2 &\lesssim \int_T (G_h + \Delta(\mathbf{I}_h \chi) - 2\epsilon^{-2}(|\mathbf{I}_h \Psi|^2 \mathbf{I}_h \chi + 2(\mathbf{I}_h \Psi \cdot \mathbf{I}_h \chi) \mathbf{I}_h \Psi - \mathbf{I}_h \chi)) \cdot \rho_T \, dx \lesssim \int_T (G_h - G) \cdot \rho_T \, dx \\ &\quad + A_T(\chi - \mathbf{I}_h \chi, \rho_T) + C_T(\chi - \mathbf{I}_h \chi, \rho_T) + 3(B_T(\Psi, \Psi, \chi, \rho_T) - B_T(\mathbf{I}_h \Psi, \mathbf{I}_h \Psi, \mathbf{I}_h \chi, \rho_T)) \end{aligned} \quad (\text{A.20})$$

The last term on the right hand side of (A.20) is estimated using (3.7), Lemmas 3.4 and 3.8(iii).

$$\begin{aligned} B_T(\Psi, \Psi, \chi, \rho_T) - B_T(\mathbf{I}_h \Psi, \mathbf{I}_h \Psi, \mathbf{I}_h \chi, \rho_T) &= B_T(\Psi, \Psi, \chi - \mathbf{I}_h \chi, \rho_T) + B_T(\Psi, \Psi, \mathbf{I}_h \chi, \rho_T) \\ &\quad - B_T(\mathbf{I}_h \Psi, \mathbf{I}_h \Psi, \mathbf{I}_h \chi, \rho_T) \lesssim \epsilon^{-2} h_T^\alpha \|\Psi\|_{1+\alpha}^2 \|\chi\|_{1+\alpha} \|\rho_T\|_h. \end{aligned} \quad (\text{A.21})$$

The first term of the right hand side of (A.20) is estimated using Hölder's inequality, the second and third terms are estimated using Hölder's inequality, Lemma 3.4, (A.4), similar to the corresponding terms in Lemma 3.9. Then a combination of (A.21), Lemma A.4, and the regularity result (3.14) yields the first inequality in Lemma 3.12. Define

$$\rho_E := \begin{cases} [\nabla(\mathbf{I}_h \chi) \nu] b_E & \text{in } \omega_E, \\ 0 & \text{in } \Omega \setminus \omega_E. \end{cases}$$

To find the second estimate in Lemma 3.12, the same technique in Lemma 3.9 is utilized. Here, we add and subtract $\sum_{T \in \omega_E} \int_T 2\epsilon^{-2}(|\mathbf{I}_h \Psi|^2 \mathbf{I}_h \chi + 2(\mathbf{I}_h \Psi \cdot \mathbf{I}_h \chi) \mathbf{I}_h \Psi + \mathbf{I}_h \chi) \cdot \rho_E \, dx$ instead and use (3.13) to obtain

$$\begin{aligned} \|\boldsymbol{\eta}_E\|_{0,E}^2 &\lesssim \int_E [\nabla(\mathbf{I}_h \chi) \nu] \cdot \rho_E \, ds = \sum_{T \in \omega_E} \left(\int_T (G + \Delta(\mathbf{I}_h \chi) - 2\epsilon^{-2}(|\mathbf{I}_h \Psi|^2 \mathbf{I}_h \chi + 2(\mathbf{I}_h \Psi \cdot \mathbf{I}_h \chi) \mathbf{I}_h \Psi - \mathbf{I}_h \chi)) \cdot \rho_E \, dx \right. \\ &\quad \left. + A_T(\mathbf{I}_h \chi - \chi, \rho_E) + C_T(\mathbf{I}_h \chi - \chi, \rho_E) + 3(B_T(\mathbf{I}_h \Psi, \mathbf{I}_h \Psi, \mathbf{I}_h \chi, \rho_E) - B_T(\Psi, \Psi, \chi, \rho_E)) \right). \end{aligned} \quad (\text{A.22})$$

Use Hölder's inequality and first part of Lemma 3.12 to estimate the first term of the right hand side of (A.22). The second and third terms are estimated analogous to the corresponding terms in Lemma 3.9 along with (A.4) and (3.14). Follow similar proof in (A.21) with (A.4) to estimate the last term in (A.22). \square